6. A Reduction Catalyst Powered by Its Own 10-Electron Battery: Synthesis and Properties of a Pentaviologen-Linked Corrinatocobalt Complex

by **Beat Steiger** and **Lorenz Walder***

Institut für Organische Chemie, Universität Bern, Freiestr. 3, CH–3012 Bern

Dedicated to Prof. *Rolf Scheffold* on the occasion of his 60th birthday

(7.XI.91)

The synthesis and properties of the molecular reduction device **7b** (Co^{II}–V$_5^{++}$) consisting of a reduction catalyst (a derivative of vitamin B$_{12}$, Co^{II}) and a covalently linked 10-electron reservoir (five viologen units, V^{++}) is described. The five viologen subunits were introduced at C(2) and C(3) of the side chains *c* and *g* and *b*, *e* and *f*, respectively, of an appropriate derivative of heptamethyl cob(III)yrinate by *N*-alkylation of 1-methyl-4,4′-bipyridinium iodide (see *Scheme*). The pentaviologen-linked corrinatocobalt(II) complex **7b** behaves as a molecular electron trap with respect to the Co^{III}/Co^{II} redox couple. The phenomenon is related to the structural and thermodynamic relation of the corrin and viologen subunits in **7b**, *i.e.* the relative redox energies and the spherical inner-outer arrangement of the two types of redox systems. When completely reduced to Co^{I}–V$_5^{0}$, **7b** exhibits multiple reductive elimination of *trans*-1,2-dibromocyclohexane to cyclohexene under concomitant oxidation to Co^{II}–V$_5^{++}$. Rate measurements indicate that the reduction occurs *via* Co^{I} which is regenerated by intramolecular electron transfer from the periphery of the molecule, *i.e.* by V^{0} and V$^{+\cdot}$.

1. Introduction. – Reversible storage of several electrons in a single organic molecule or coordination compound can be achieved in two ways. Either the electrons are stored in the closely spaced energy levels of an extended π-system [1] or in the electronically decoupled electroactive subunits of an oligomeric redox system [2]. Examples of the first type of *electron sponges* display sequential one- or two-electron reduction steps at increasingly negative potentials, whereas those belonging to the second type show single multi-electron reductions at the potential of the corresponding monomer, provided that the redox centers do not interact [3]. The main objectives in the area are the optimization of charge and energy stored per molecular weight and the rate and thermodynamics of (dis)charging, *i.e.* they are related to battery research.

Another subject of relevance to our work is the *multi-electron reduction catalysis*, *i.e.* the transfer of several electrons upon a catalyst-substrate collision eventually in one elementary step. Impressive examples are the face-to-face porphyrins which were originally designed to electro-catalyze the 4-electron reduction of O_2 to 2 H_2O by double-coordination of O_2 and concomitant 4-electron injection [4]. The face-to-face porphyrins are used as surface-adsorbed electrocatalysts. They do not need to dispose of a 4-electron reservoir, but rather guide the electrons from the electrode onto the metalloporphyrin-complexed O_2.

Finally and again related to our work are electron acceptor/donor-linked photosensitizers which were proposed as model photosynthetic systems [5]. Typically, monoviologen-linked or -capped (metallo)porphyrins quench the fluorescence by photoinduced electron transfer [6]. Improved quenching efficiencies were reported for some tetraviologen-linked porphyrins [7]. From our point of view, the latter compounds may also be looked at as an electron reservoir – although empty – linked to a (photo)catalyst.

To the best of our knowledge, no organic electron sponge has yet been covalently linked with a reduction catalyst in order to realize multi-electron reduction catalysis or multiple one(or two)-electron reductions so far. We recently reported on a binuclear Co–Ru reduction catalyst with an energy-converting subunit [8]. We describe now the synthesis (**1a** → **2** → **3** → **5a** → **7b**) and properties of the molecular reduction device **7b** consisting of a 10-electron sponge linked covalently to a vitamin-B_{12}-based reduction catalyst (*Fig. 1*, *Scheme*). When completely reduced, **7b** brings about multiple reductive

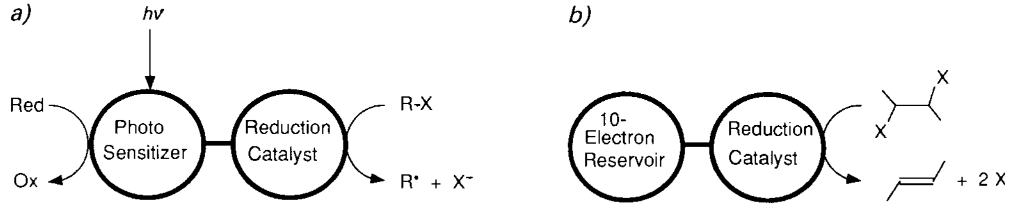

Fig. 1. *Molecular reduction devices. a*) Reduction catalyst covalently linked to an energy-conversion subunit [8]; *b*) reduction catalyst covalently linked to an electron sponge (this work).

Scheme

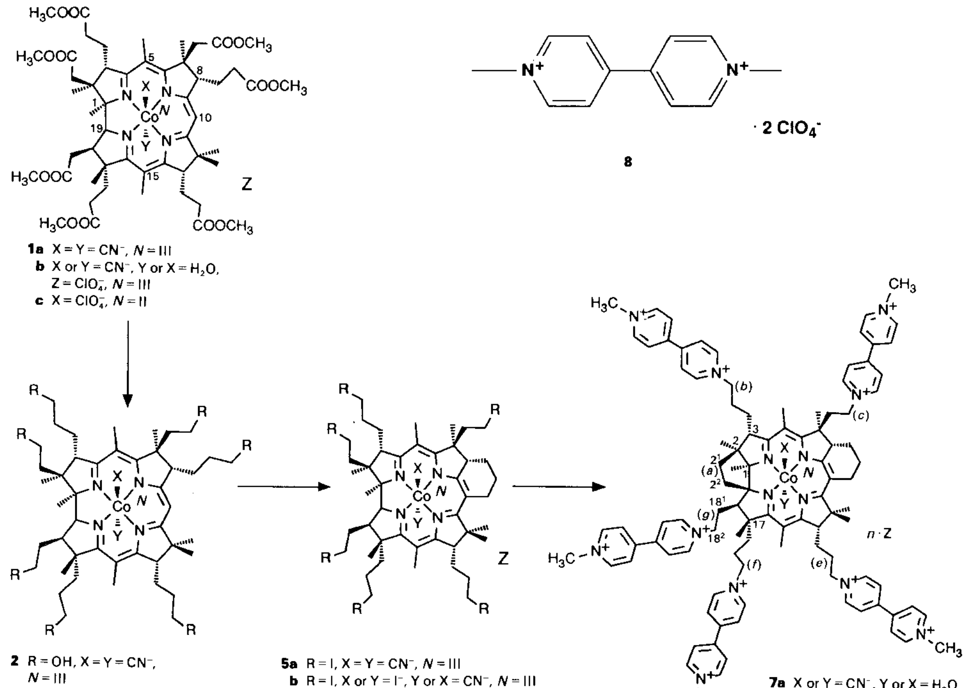

8 $\cdot 2\,ClO_4^-$

1a $X = Y = CN^-$, $N = III$
b X or $Y = CN^-$, Y or $X = H_2O$, $Z = ClO_4^-$, $N = III$
c $X = ClO_4^-$, $N = II$

2 $R = OH$, $X = Y = CN^-$, $N = III$
3 $R = CH_3SO_3$, $X = Y = CN^-$, $N = III$
4 $R = I$, $X = Y = CN^-$, $N = III$

5a $R = I$, $X = Y = CN^-$, $N = III$
b $R = I$, X or $Y = I^-$, Y or $X = CN^-$, $N = III$
6a $R = CH_3COO$; $X = Y = CN^-$, $N = III$
b $R = CH_3COO$, X or $Y = CN^-$, Y or $X = H_2O$, $Z = ClO_4^-$, $N = III$
c $R = CH_3COO$, X or $Y = ClO_4^-$, $N = II$

7a X or $Y = CN^-$, Y or $X = H_2O$, $n = 11$, $Z = Cl^-$, $N = III$
b X or $Y = ClO_4^-$, Y or $X = H_2O$ (or DMF), $n = 10$, $Z = ClO_4^-$, $N = II$

eliminations of a vicinal dihalide, as expected. However, we were quite surprised to find that **7b** shows the properties of a *molecular electron trap*, a phenomenon so far unknown on a molecular level.

2. Synthesis. – Heptamethyl dicyanocob(III)yrinate (**1a**) and its axial coordination derivatives are available from vitamin B_{12} by known procedures [9][1]). The seven MeO groups in **1a** or NHR groups in vitamin B_{12} can be replaced by RO *via* cobyrinic acid [11] or by direct esterification of vitamin B_{12} according to *Kräutler* and coworkers [11] and *Murakami et al.* [12], respectively. Eventually, such a procedure was applied in this work in order to extend the seven side chains of the corrin system with redox-active subunits *via* ester linkages. However, as *i*) intramolecular electron transfer depends crucially on the distance between the redox sites and *ii*) esters are prone to solvolysis, a structure with spacers as short and chemically as resistant as possible was envisaged. Introducing the reaction sequence **1a** → **2** → **3**, another approach to a vitamin-B_{12} derivative with the potential of further transformation of the seven side chains was opened by *Gossauer* and coworkers [13]. According to our original synthesis plan, exchange of all mesylate moieties in **3** by I-atoms followed by persubstitution with 1-methyl-4,4′-bipyridinium iodide should lead to a heptaviologen derivative of the corrin system.

Starting from cobester **1a**, the heptol **2** was prepared according to [13], but additionally purified by reversed-phase chromatography and identified spectroanalytically before further use (*cf. Exper. Part*). Then **2** was transformed into **3** using a modified procedure of [13] (*cf. Exper. Part*). Heating **3** under reflux in NaI/butan-2-one for 15 min gave, after reaction with HCN and chromatography on silica gel, in 77% yield the corresponding heptaiodide **4** (*cf. Exper. Part*). The reaction of **4** with an excess of 1-methyl-4,4′-bipyridinium iodide [14] yielded a mixture of violet and blue corrinoids, which could not be separated by conventional methods. Heating **3** under reflux in NaI/butan-2-one for 8 h followed by reaction with HCN and chromatography on silica gel yielded the blue corrinoid **5a** (85%) as determined by spectroscopic methods (*cf. Exper. Part*). Under the same conditions, **5a** was also obtained from the heptaiodide **4** in 82% yield. Intramolecular electrophilic substitution took place leading to ring formation between the corrin C(10) and the *d*-side chain $C(8^3)$ confirming the known reactivity of C(10) towards electrophilic reagents [15]. The structure of **5a** was further supported by spectral analysis of the corresponding, more stable hexaacetate **6a** obtained by the mild chemical transformation **5a** → **6a** (*cf. Exper. Part*).

The UV/VIS spectra and the IR absorption bands (1490–1650 cm^{-1}) of **5a** and **6a** show a distinct similarity to that of heptamethyl *Coα,Coβ*-dicyano-10-methylcob(III)yrinate [15]. The ^1H-NMR spectra of the heptaiodide **4** and a heptaacetate derivative [13] as compared to that of **5a** and **6a** reveal the substitution of the H-atom at C(10) in **5a** and **6a** by the absence of the signal of H–C(10) at 5.48 and 5.49 ppm, respectively. Additionally, in the ^{13}C-NMR spectra, the C(10) signal ist shifted from 90.8 (*d*; **4**) and 90.3 ppm (*d*; heptaacetate [13]) to 103.1, 103.6, or 104.7 ppm (3*s*; 2*s* are assigned to C(5) and C(15); **5a**) and to 101.6 or 101.7 ppm (2*s*; 1*s* is assigned to C(5); **6a**), respectively. A detailed NMR analysis of **6a** led unambiguously to the proposed structure. Particularly, the constitution at C(10) was deduced after most of the signals were assigned by $^1H,^1H$ (COSY, 1D-TOCSY, and ROESY) and heteronuclear (^1J(C,H) and ^nJ(C,H) COSY) 2D-NMR measurements (*cf. Exper. Part*) from the ROE's observed between the protons at $C(8^3)$ and the 2 Me groups at C(12) as well as the coupling pattern of the protons at C(8), $C(8^1)$, $C(8^2)$, and $C(8^3)$.

---

[1]) For the nomenclature of corrins, see [10].

The dicyanocobalt complex **5a** was then transformed into the (cyano)iodocobalt complex **5b** in order to prevent side reactions of a dissociating CN^- ion from **5a** in the following reaction step (*cf. Exper. Part*). The reaction of **5b** with 1-methyl-4,4′-bipyridinium iodide yielded, after ion exchange and chromatography on *XAD*, as the main product (49%) a red corrinoid for which structure **7a** is proposed. A further cyclization – now between the corrin C(19) and the α-side chain C(2^2) – seems to compete favorably with the envisaged intermolecular S_N2 reaction, even if a large excess of 1-methyl-4,4′-bipyridinium iodide ($c > 0.3$M) was used (*cf. Exper. Part*). We do not know of a precedent pointing to the reactivity observed for C(19). However, electron transfer from the corrin moiety to a bipyridinium subunit in **7a** may play a role in this unique reaction.

The UV/VIS spectrum of **7a** is dominated by the strong absorption of the bipyridinium subunits at 262 nm. Absorptions of the corrin part of **7a** show up as the weak γ- and α-bands at 366 and 550 nm, respectively. In the range of 328 to 700 nm, the spectrum of **7a** is very similar to that of **6b**. Over the whole absorption range, it can be simulated with a 5:1 mixture of viologen and **6b**. The presence of five bipyridinium subunits is also clearly shown by the ^{1}H- and ^{13}C-NMR spectra. There is no evidence for a mixture of axial coordination isomers. In the ^{13}C-NMR spectra of **7a**, the 2*s* occurring at 80.1 and 85.9 ppm are assigned to C(1) and C(19) giving a first indication of the proposed structure. The constitution and configuration at C(19) is supported, after complete assignment of all signals from the CH and Me groups in the molecule by 2D-NMR spectroscopy (^1J(C,H) COSY and ROESY), on the ground of the ROE's and ^{1}H,^{1}H correlations observed between the side chains *a* and *g* (*cf. Exper. Part*).

For the purpose of further electrochemical and spectroelectrochemical investigations, **7a** was transformed into the CN-free (pentaviologen-corrinato)cobalt(II) complex **7b** by repetitive electrochemical adsorption/dissolution of the completely reduced complex (Co^I—V_5^0) from DMF/H_2O/electrolyte onto a carbon-felt cathode (*cf. Exper. Part*).

3. The (Pentaviologen-corrinato)cobalt(II) Complex 7b, a Molecular Electron Trap. – The redox chemistry of the (pentaviologen-corrinato)cobalt(II) **7b** (Co^{II}—V_5^{++}) was studied by electrochemical techniques and compared with that of its free subunits using the (hexaacetoxy-corrinato)cobalt(II) **6c** and 1,1′-dimethyl-4,4′-bipyridinium diperchlorate (= methylviologen; **8**; V^{++}) as reference molecules. At very low concentrations of **7b** ($c < 0.1$ mM), i_p *vs.* v plots obtained from cyclic voltammetry (CV) in dimethylformamide (DMF)/(Bu_4N)ClO_4 tend to be linear and indicate adsorption of the molecule on the electrode surface. At higher concentrations, the diffusional contribution dominates the current response. It is possible to adsorb the completely reduced complex **7b** (Co^I—V_5^0) by bulk electrolysis on a large electrode surface if the mixed solvent/electrolyte water DMF/(Bu_4N)ClO_4 is used. No indication for adsorption is found for the $V^{++}/V^{\cdot+}$ couple of **8** by CV in DMF/(Bu_4N)ClO_4. The $V^{++}/V^{\cdot+}$ and the $V^{\cdot+}/V^0$ reduction and oxidation waves observed by CV in DMF/(Bu_4N)ClO_4 for **7b** and **8** are very similar indicating no association of $V^{\cdot+}$ subunits in **7b** which might be expected from the behavior of oligomeric viologens [2]. The viologen subunits in **7b** behave as *multiple non-interacting redox sites* (an important condition for the 'battery effect' to be discussed in the following chapter) as the observed $E_{1/2} = (E_{pc} + E_{pa})/2$ involving the 5 viologen subunits in **7b** is essentially identical with that of a single redox site in **8** [3] (*Table 1*).

To simulate the redox behavior of **7b** (Co^{II}—V_5^{++}) as close as possible, its electrochemistry was compared with that of 1:5 mixtures of the subunits models **6c** (Co^{II}) and **8** ($5V^{++}$) (*Fig. 2*). The Co^{III}/Co^{II} redox couple shows the intensity expected for a slow redox system at low concentration in the 1:5 mixture. Under the same conditions, no Co^{III}/Co^{II}

Table 1. *Site-Specific Reduction Potentials of the (Pentaviologen-corrinato)cobalt(II) Complex* **7b** *and Its Reference Molecules* **6c** *and* **8**

	Redox couple			
	Co^{III}/Co^{II}	$V^{++}/V^{\cdot+}$	Co^{II}/Co^{I}	$V^{\cdot+}/V^{0}$
6c	+0.38[a])		−0.49[b])	
1c	+0.39[a])		−0.52[b])	
8		−0.43[b])		−0.81[b])
7b	+0.31[a])	−0.40[b])	*ca.* −0.5[c])	−0.82[b])

[a]) From spectroelectrochemistry.

[b]) From CV.

[c]) Estimated from spectroelectrochemistry.

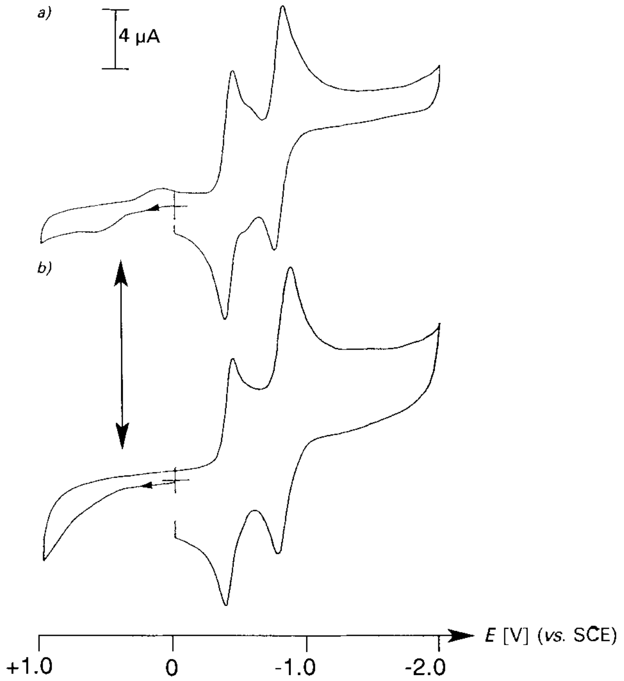

Fig. 2. *Cyclic voltammetry* a) *of the subunit models* **6c**/**8** *and* b) *of* **7b** *in DMF/(*Bu_4N*)*ClO_4 (0.1 M). v = 0.05 V/s at a glassy carbon electrode; *a*) 1:5 mixture of **6c** (0.25 mM) and **8** (1.25 mM); *b*) **7b** (*ca.* 0.25 mM).

reduction and oxidation waves are observed for **7b**. Two reasons may by responsible for this behavior. Either the thermodynamic Co^{III}/Co^{II} reduction potential is shifted in negative direction due to coordination of a Co^{III}-stabilizing axial ligand and the current response is hidden by the viologen subunits, or, the rate of electron transfer to and from Co through the viologen environment is too slow to be observed on the time scale of CV.

Using spectroelectrochemistry (*cf. Exper. Part*), a technique that allows a slow redox couple to equilibrate with the electrode potential, it was possible to determine the VIS spectra of Co^{III}–V_5^{++}, Co^{II}–V_5^{++}, Co $^{II/I}$–$V_5^{+\cdot}$, and Co^{I}–V_5^{0}. From the potential-dependent

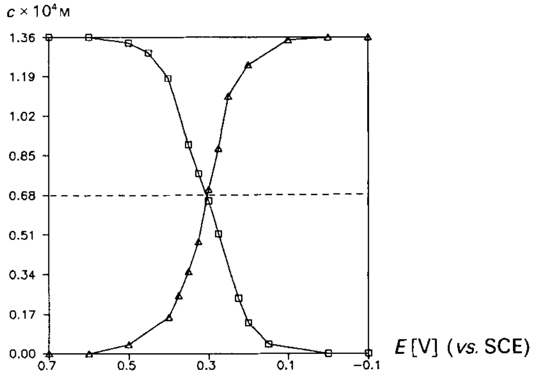

Fig. 3. *Determination of the* Co^{III}/Co^{II} *reduction potential in* **7b** *by spectroelectrochemistry.* □: stepwise reduction of $Co^{III}–V_5^{++}$; △: stepwise oxidation of $Co^{II}–V_5^{++}$, concentration analysis from absorption at 358 and 316 nm. [**7b**] ≈ $1.4 \cdot 10^{-4}$ M, equilibration time *ca.* 30 min/step.

spectral transition $Co^{III}–V_5^{++} + e^- \rightleftharpoons Co^{II}–V_5^{++}$ (30 min equilibration time for each potential step), $E^0(Co^{III}/Co^{II}$; **7b**$) = 0.31$ V (*vs.* SCE) resulted (*Fig. 3*). This value is just slightly more negative than $E^0(Co^{III}/Co^{II}$; **6c**$) = 0.38$ V. Thus, the fact that no current is observed in CV is definitely related to slow kinetics.

It is possible to measure this slow rate, at least qualitatively. Under the bulk-electrolysis conditions present in the spectroelectrochemical cell (*cf. Exper. Part*), *Eqns. 1* and *2* govern the concentration change for a potential step over E^0 into the diffusion-limited current range.

$$c_t = c^0 \cdot e^{-kt} \tag{1}$$

c_t: concentration at time t, c^0: concentration at $t = 0$; k: rate

$$k = A \cdot D \cdot V^{-1} \cdot \delta^{-1} \tag{2}$$

A: electrode surface; D: diffusion coefficient; V: cell volume; δ: diffusion layer thickness. For a diffusion-limited electrochemical reduction (or oxidation), k (or $t_{1/2}$) is only a function of the cell characteristics (A,V,δ) and the diffusion coeffient (D). Potential steps over the known E^0 of the redox couples present in the 1:5 mixture **6c**/**8** yielded $t_{1/2}$ values for the $V^{++}/V^{+\cdot}$ reduction and oxidation and the Co^{III}/Co^{II} oxidation of 2 and 3 min, respectively (*Table 2*). As **8** is a fast redox couple under the conditions of CV, 2 min for bulk electrolysis reflects the cell characteristics tuned by the diffusion coefficient; 3 min for $Co^{III} \rightarrow Co^{II}$ of **6c** (slow under conditions of CV) is due to a small diffusion coefficient rather than slow kinetics (see below). Still in case of the 1:5 mixture, $t_{1/2}$ of the reduction $Co^{III} + e^- \rightarrow Co^{II}$ depends strongly on the end potential of the cathodic potential step. If $E_{end} = -0.2$ V, the diffusion-controlled rate is observed ($t_{1/2} = 3$ min), but if $E_{end} = -0.65$ V, then $t_{1/2} < 0.25$ min results. In the latter case, catalysis *via* $V^{+\cdot}$ is involved. Generally, the same behavior is observed for the (pentaviologen-corrinato)cobalt(II) **7b** ($t_{1/2}$ is slightly larger, probably because of its smaller diffusion coefficient). However, if the potential is stepped to +0.5 V, after equilibration of a solution of $Co^{II}–V_5^{++}$ at −0.2 V, very slow oxidation with $t_{1/2} = 11$ min is observed (to be compared with $t_{1/2} = 3$ min for the 1:5 mixture, *Table 2*, *Fig. 4*).

The different rate of Co^{II} oxidation in **7b** and **6c**/**8** is definitely related to the structure of **7b** and its interaction with an electrode surface as compared to that of the free subunits in the 1:5 mixture. In case of the mixture, the subunits exchange electrons with the

Table 2. *Kinetics of Reduction and Oxidation of the Redox Subunits in* **7b** *and of the Free Redox Systems* **6c/8** *from Spectroelectrochemistry*

Redox system[a])	Potential step E [V] *vs.* SCE	Oxidation states involved	$t_{1/2}$ [min]	Conc. change analyzed at λ [nm]
7b	+0.5→−0.2	$Co^{III}-V_5^{++} \rightarrow Co^{II}-V_5^{++}$	4	358 (Co^{III})
6c/8	+0.5→−0.2	$Co^{III}/5V^{++} \rightarrow Co^{II}/5V^{++}$	3	358 (Co^{III})
7b	+0.5→−0.65	$Co^{III}-V_5^{++} \rightarrow Co^{II}-V_5^{++}$	< 0.25	358 (Co^{III})
7b	+0.5→−0.65	$Co^{II}-V_5^{++} \rightarrow Co^{II/I}-V_5^{+\cdot}$[b])	3	610 ($V^{\cdot+}$)
6c/8	+0.5→−0.65	$Co^{III}/5V^{++} \rightarrow Co^{II}/5V^{++}$	< 0.25	358 (Co^{III})
6c/8	+0.5→−0.65	$Co^{II}/5V^{++} \rightarrow Co^{II/I}/5V^{+\cdot}$[b])	2	610 ($V^{\cdot+}$)
7b	−0.65→−0.2	$Co^{II/I}-V_5^{+\cdot} \rightarrow Co^{II}-V_5^{++}$[b])	3	610 ($V^{\cdot+}$)
6c/8	−0.65→−0.2	$Co^{II/I}/5V^{+\cdot} \rightarrow Co^{II}/5V^{++}$[b])	2	610 ($V^{\cdot+}$)
7b	−0.2→+0.5	$Co^{II}-V_5^{++} \rightarrow Co^{III}-V_5^{++}$	**11**	316 (Co^{II})
6c/8	−0.2→+0.5	$Co^{II}/5V^{++} \rightarrow Co^{III}/5V^{++}$	**3**	322 (Co^{II})

[a]) [**7b**] = 0.048 mM; [**6c**] = 0.048 mM; [8] = 0.24 mM. Other experimental conditions, see *Fig. 8*.

[b]) The portion of Co^{I} was not determined.

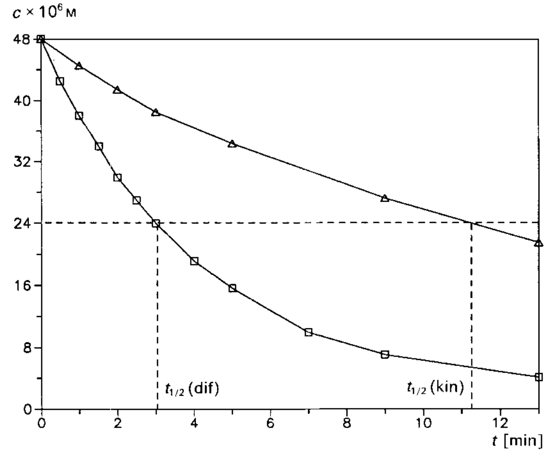

Fig. 4. *Concentration* vs. *time behavior upon potential step showing slow kinetics of* Co^{II} *oxidation in* **7b** *as compared to* **6c**. Potential step −0.2→+0.5 V for △: **7b**; □: **6c/8** 1:5.

electrode independent from each other according to the rules of thermodynamics and kinetics. However, in the (pentaviologen-corrinato)cobalt(II) **7b**, only the viologen subunits come into close contact with the electrode, provided that the space-demanding $V^{+\cdot}$ subunits envelop the corrin moiety tightly (*Fig. 5*). According to this model, heterogeneous electron transfer to or from Co has to involve a viologen subunit as a 'bridge'. A lower limit for the activation barrier of 710 mV (16.4 kcal/mol) for oxidation results from the relative redox levels of the central Co^{II} and the outer sphere (V^{++}) retarding the Co^{II} oxidation dramatically. This barrier is expected to be independent of the electrode potential, and absolute-rate theory predicts a rate constant in the range of 0.1 to 10 s^{-1} (depending on the choice of the preexponentional factor), *i.e.* a slightly larger k than experimentally observed. The self-exchange rate for electron transfer in the Co^{III}/Co^{II} couple of **6c** is small because of coodination/decoordination kinetics of solvent/electrolyte species at the axial Co^{III} positions. If similar reactions are coupled with electron transfer in case of **7b**, an additional barrier of 1 to 3 kcal may be active even at such a

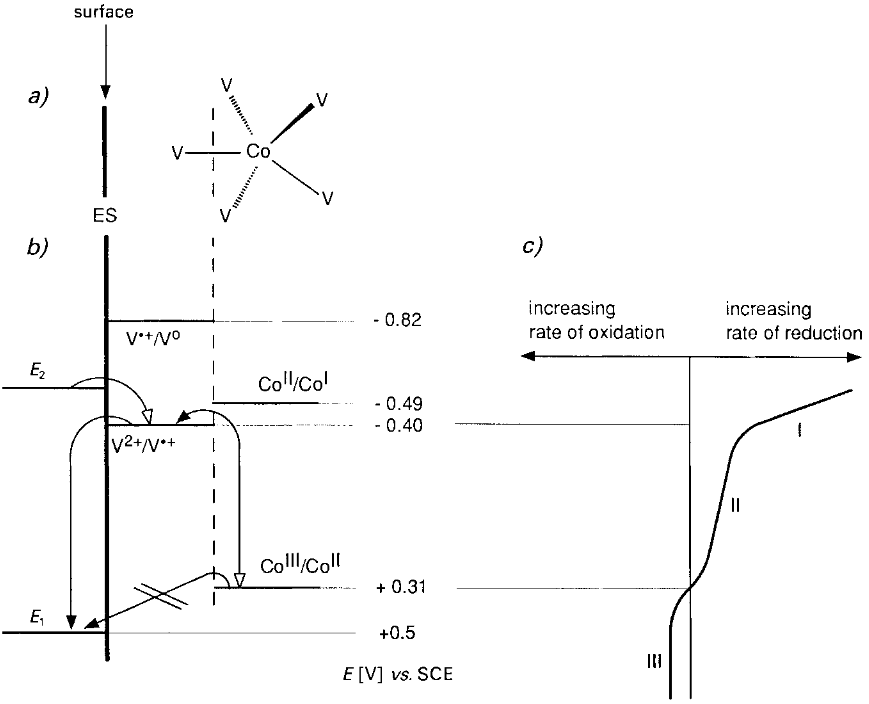

Fig. 5. *The electron-trap mode of action: a)* Pseudo-spherical arrangement of the outer viologen subunits (V) around the central [Co(corrinato)]entity (Co) in **7b** forcing the interaction with an electrode surface to be always ES-V-Co, *i.e.* independent of rotation of **7b**. *b)* Fixed redox potentials of the inner (Co) and outer (V) electroactive subunits in **7b**. Intramolecular and heterogeneous electron transfers: $Co^{II}-V_5^{++}$ in solution with the tunable electrode potential $E = E_1 = +0.5$ V (activation barrier: 710 mV); $Co^{III}-V_5^{++}$ in solution with $E = E_2 = -0.65$ V. *c)* Electrode potential dependent rate of all-over Co^{III} reduction and Co^{II} oxidation of a solution of **7b** with $[Co^{III}-V_5^{++}] = [Co^{II}-V_5^{++}]$; I: V-catalyzed reduction; II: reduction with potential-dependent activation barrier; III: oxidation with potential-independent barrier.

positive ΔG (ΔG with respect to the reaction $V^{++}-Co^{II} \rightarrow V^{+}-Co^{III}$). The reduction $Co^{III} + e^{-} \rightarrow Co^{II}$ is 'catalyzed' by the viologen subunits if the electrode potential (E) is in the neighborhood of −0.4 V or more negative, but it will be slowed down by an activation barrier depending on the electrode potential for $+0.3 > E > -0.3$ V.

In recent years, the charge trapping and current rectifying abilities of modified electrodes were thoroughly investigated. The principle is based on two electroactive layers with different reduction potentials, *e.g.* $E_1^0 < E_2^0$ placed as two layers onto an electrode surface [16]. Vectorial electron transfer takes place from the reduced and more reducing layer (with E_1^0) to the oxidized layer exhibiting E_2^0. In case of the modified electrode, the vectorial electron transfer is essentially a one-dimensional problem, *i.e.* it can be realized by the linear assembly:

electrode – redox polymer 1 – redox polymer 2

However, if the charge-trapping phenomenon has to occur between an electrode and a freely diffusing and rotating particle, the problem becomes 3-dimensional, and its most general realization is a spherical arrangement with the two types of redox centers placed on an outer and an inner layer. The (pentaviologen-corrinato)cobalt(II) **7b** is the first synthetic example that has been shown to fulfill these structural and thermodynamic conditions as a molecular entity with functional subunits that add up to the charge-trapping phenomenon. We have observed it by electrochemical techniques, but it may definitely occur in homogeneous electron-transfer reactions, provided the partner interacts only with the surface of **7b**. The principle described may play a key role in the charging and discharging processes of redox proteins, or – more specifically – it may explain how the reducing power of a redox protein can be stocked in an oxidizing environment and how vectorial electron transfer into the core of a molecule can be guided by electroactive subunits.

4. The (Pentaviologen-corrinato)cobalt(II) 7b, a Reduction Catalyst Powered from Its Own Battery. – Cob(I)alamin and related macrocyclic Co^{I} complexes ('Co^{I}') are well known to catalyze the reductive generation of alkyl (acyl) radicals from alkyl halides (carboxylic anhydrides) as well as the reductive elimination of vicinal leaving groups [17]. These reactions consume one or two electrons which are originally supplied by a reducing metal or by the cathode of an electrochemical cell. The role of the 'Co^{I}' catalyst is twofold: It carries the electrons into the solution, and it exhibits there high reactivity towards the electrophilic substrates. It is important to realize that the same d_{z^2}-orbital of Co is responsible for both, the storage of the electron and the reactivity. With (pentaviologen-corrinato)cobalt(II) **7b**, we envisaged a *molecular task-sharing system* with respect to electron storage (10 electrons in the 5 viologen subunits) and reactivity (Co^{I}), assuming that efficient intramolecular electron transfer from the peripheral electron reservoir to Co occurs.

Preliminary studies with **7b** and different alkyl halides showed that the charge-storing capacity quickly degrades if radicals are generated. The viologen subunits and the corresponding cation radicals are prone to radical attack and loose their redox activity, due to reactions probably related to the α-H substitution by alkyl radicals in case of the methylpyridinium ion [18] and the well known coupling of alkyl radicals with aromatic anion radicals [19]2). The following studies on the performance of **7b** were, therefore, done on a reaction involving no free radicals, *i.e.* the reduction of *trans*-1,2-dibromocyclohexane ($C_6H_{10}Br_2$) to cyclohexene (C_6H_{10}). The standard reduction potential $E^0(C_6H_{10}Br_2) = 0.125$ V *vs.* SCE for *trans*-1,2-dibromocyclohexane + $2e^- \rightarrow$ cyclohexene was estimated from thermochemical data and some approximations with respect to solvation [20]. The reduction potentials reported in *Table 1* for the V^0,Co^{I} and V$^{+\cdot}$ subunits models **8** and **6c** as well as the corresponding subunits in **7b** are all more negative than $E^0(C_6H_{10}Br_2)$ predicting complete discharge of $Co^{I}–V_5^0$ to $Co^{II}–V_5^{++}$ and concomitant transformation of 5.5 $C_6H_{10}Br_2$ to 5.5 C_6H_{10} per 1 $Co^{I}–V_5^0$ at equilibrium. If **7b** was reduced to $Co^{I}–V_5^0$ ($c \approx 5 \cdot 10^{-5}$ M) in the spectroelectrochemical cell and then a 100-fold excess of $C_6H_{10}Br_2$ was added (under open-circuit conditions), the V$^{+\cdot}$ absorption appeared as a transient indicating $Co^{I}–V_5^0 \rightarrow Co^{II}–V^{+\cdot} \rightarrow Co^{II}–V_5^{++}$. This happened within mixing time (0–3 s), and only a lower limit of the rate was available. GC Analysis of the

---

2) This is definitely a severe restriction and limits the scope of applications of **7b** to processes involving no free radicals, *e.g.* reductive eliminations. It indicates that organic one-electron redox systems need efficient protection in order to persist as a rechargeable electron sponge in presence of alkyl radicals.

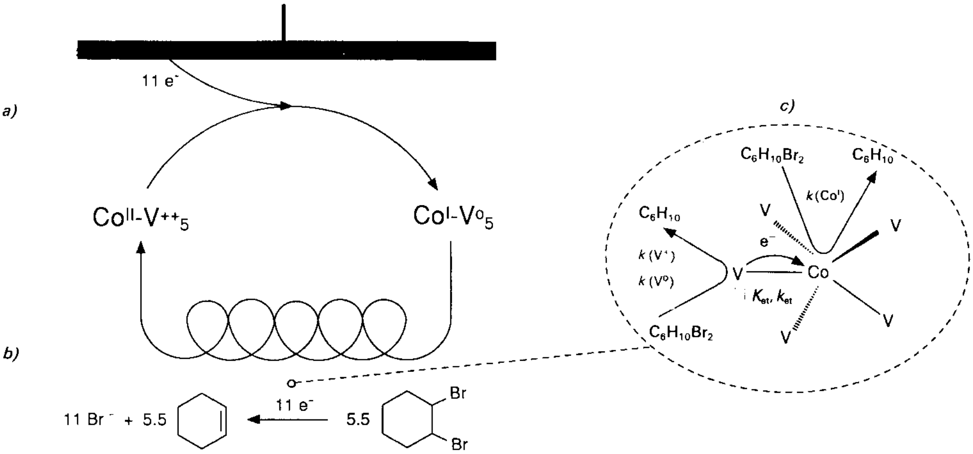

Fig. 6. *Multiple 2-electron reduction:* a) *11-electron charging,* b) *multiple substrate conversion, and* c) *task sharing* (site of electron storage and of catalysis based on relative rates)

reaction mixture confirmed the formation of cyclohexene (*a*) and *b*) as two sequential steps in *Fig. 6, cf. Exper. Part*). If **8** as V^0 or V^{+} was used instead of $Co^I{-}V_5^0$ under similar conditions, very slow oxidation of the electron donors was observed. In case of a mixture of the catalysts **8** and **6c**, the reaction $V^0 \to V^{+} \to V^{++}$ occurred again within mixing, except for the very end of the reaction where some retardation showed up.

Accurate 2nd-order rate constants of the $C_6H_{10}Br_2$ reduction by the free subunit **8** ($k(V^+)$,$k(V^0)$) were measured by such time-resolved VIS spectroscopy and/or electrochemical techniques (*cf. Exper. Part*). The rate of oxidation of **6c** ($k(Co^I)$) by $C_6H_{10}Br_2$ was determined from the plateau-current observed by linear-scan voltammetry (LSV) (*Fig. 7b*) [21]. All rates are reported in *Table 3*. It is interesting to note that the relative

Table 3. *Rate of Dibromocyclohexane Reduction by the Subunit Models* **8** *and* **6c**

	Co^{II} **6c**	$V^{\cdot+}$ **8**	Co^I **6c**	V^0 **8**
E^0 [V] *vs.* SCE	+0.38	−0.43	−0.49	−0.81
$k_{1(\mathrm{red})}$[a]) [$\mathrm{M}^{-1}\mathrm{s}^{-1}$]	no reaction	$8 \cdot 10^{-3}$	$4.1 \cdot 10^4$	1

[a]) Conditions, see *Exper. Part.*

($k(V^0)/k(V^+) = 125$) and absolute k values of V^0 and V^+ fit well an extrapolation of the *Marcus*-type rate *vs.* driving-force relation reported recently by *Savéant et al.* for the same substrate but stronger outer-sphere electron donors [20]. The rate observed for the (corrinato)cobalt(I) complex of **6c** is orders of magnitude larger ($k(Co^I)/k(V^0) = 4.1 \cdot 10^4$) inspite that $E^0(Co^{II}/Co^I)$ is located in-between $E^0(V^{++}/V^{+})$ and $E^0(V^{+}/V^0)$. The kinetic advantage of Co^I is explained by bonding interactions of the Co complex with $C_6H_{10}Br_2$ in the transition state as compared to the outer-sphere electron-transfer situation in case of $V^{+\cdot}$ or V^0 and $C_6H_{10}B_2$[3][4].

The relative rates $k(Co^I)$,$k(V^0)$, and $k(V^{+\cdot})$ are the basis of the intended molecular functions (catalytic center and electron reservoir) of the subunits in **7b** because the reservoir does only discharge *via* Co^I if $k(Co^I) \gg k(V^0), k(V^{+\cdot})$ (*Fig. 6c*). Another condition to be fulfilled is $k_{et} > k(V^0)\cdot[C_6H_{10}Br_2]$, $k(V^{+\cdot})\cdot[C_6H_{10}Br_2]$. From the preliminary VIS-spectroscopic experiments on the V^0 oxidation in presence and absence of **6c** (described above), we may conclude that $k_{et} > k(V^0)\cdot[C_6H_{10}Br_2]$. This is confirmed by the following LSV experiments (*Fig. 7*): Methylviologen (**8**) in presence of $C_6H_{10}Br_2$ ($c = 2.8 \cdot 10^{-2}$ M) does not show catalysis (*Fig. 7a*)[5]. The Co complex **6c** exhibits a plateau current on the Co^{II}/Co^I wave interpreted as reduction catalysis of $C_6H_{10}Br_2$ (*Fig. 7b*). Finally, a mixture of **8** and **6c** shows week catalysis on the $V^{++}/V^{+\cdot}$ and strong catalysis on the $V^{+\cdot}/V^0$ wave (*Fig. 7c*)[6].

(Pentaviologen-corrinato)cobalt(II) **7b** is definitely a much faster electrocatalyst than **6c** (*Fig. 7c*). As an electrocatalyst, it behaves similarly to the **8**/**6c** mixture, except for the onset of catalysis being located rather in the range of the Co^{II}/Co^I wave[7]. It is difficult to evaluate the rate of $C_6H_{10}Br_2$ reduction by **7b** from the catalytic current accurately. The rate is so fast that very low [**7b**] must be used, *i.e.* one has to work in a concentration range where catalysis *via* adsorbed **7b** may become important.

The essential idea leading to the synthesis of **7b** was the combination of an electron reservoir with a reduction catalyst (*Fig. 1b*). Electrocatalysis (*a–b–a–b*) in *Fig. 6*) was just the technique of choice to get an idea on some of the rate constants in *Fig. 6c*. From

---

[3] Dissociative electron transfer from electron donors ($D^{\cdot-}$) to aliphatic alkyl halides (RX) is subject to an activation barrier that is mainly due to stretching of the C–X bond of RX on the way to the transition state. The free-energy change of this reaction is given by the sum of *Eqns. 3* and *4*, *i.e.* the difference of the corresponding reduction potentials $\Delta G = -n \cdot F \cdot (E^0(RX/R^{\cdot} + X^-) - E^0(D/D^{\cdot-}))$.

$$D^{\cdot-} - e^- \rightarrow D \tag{3}$$

$$R{-}X + e^- \rightarrow R^{\cdot} + X^- \tag{4}$$

For a constant RX and a series of $D^{\cdot-}$ differing in $E^0(D/D^{\cdot-})$, the rates of reduction follow a *Marcus*-type relation ($\ln k$ *vs.* $E^0(D/D^{\cdot-})$). Higher rates than expected are generally observed for cob(I)alamin and related macrocyclic Co^I complexes ('Co^I') if $E^0(D/D^{\cdot-})$ is replaced by $E^0(Co^{II}/Co^I)$ in the above *Marcus* relation indicating that 'Co^I' does not behave as an outer-sphere reducing agent towards RX. Stabilizing interactions in the transition state, *i.e.* partial Co–C or Co–X bond formation are responsible for the increased reactivity [20].

[4] Effectively, one- and/or two-electron reduced viologens were used as reduction mediators for MeI [22], activated vicinal dibromides [23], α-halogeno-ketones [24], azobenzene [25], acrylonitrile [26], and aromatic aldehydes and ketones [27], however, at small rates.

[5] At $[C_6H_{10}Br_2] = 30$ to $900 \cdot 10^{-3}$ M, an influence of $C_6H_{10}Br_2$ on the CV response of **8** is observed (*Exper. Part*).

[6] For certain concentration ranges, *Eqn. 5* yields k_{obs} values in the range of $k(Co^I)$ if [cat] = [**8**] and i_p on the $V^{+\cdot}/V^0$ wave are used. In these cases, the rate of the intermolecular electron transfer from V^0 to Co^{II} is faster than the rate of $C_6H_{10}Br_2$ reduction. If electron transfer from $V^{+\cdot}$ would be as efficient, one would expect $i_p(V^{++}/^{+\cdot}) = 1/2 i_p(V^{+\cdot}/V^0)$ (both measured from the same base line). The fact that $i_p(V^{++}/^{+\cdot})$ in *Fig. 7c* is much smaller indicates that K_{et} and/or k_{et} affect the observed rate.

$$i_p = n \cdot F \cdot A \cdot [cat] \cdot (D \cdot k_{obs} \cdot [C_6H_{10}Br_2])^{1/2} \tag{5}$$

[7] We have currently no explanation for the onset of electrocatalysis in the range of the Co^{II}/Co^I wave rather than on the $V^{++}/V^{+\cdot}$ wave, in spite that we find fast discharge of the $Co{-}V_5^{+\cdot}$ VIS absorption under homogeneous conditions and no indication for slow heterogeneous electron transfer.

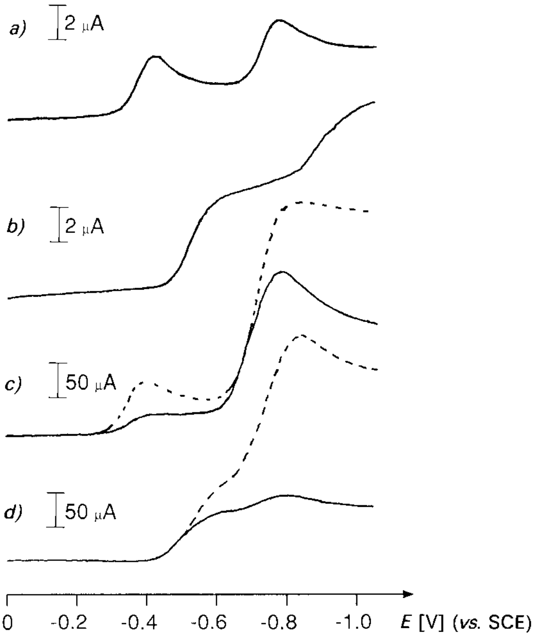

Fig. 7. *Electrocatalysis of $C_6H_{10}Br_2$ reduction with different electrocatalysts. a)* [**8**] = $0.5 \cdot 10^{-3}$ M and [$C_6H_{10}Br_2$] = 2.8×10^{-2} M; *b)* [**6c**] = $3.3 \cdot 10^{-5}$ M and [$C_6H_{10}Br_2$] = $0.6 \cdot 10^{-2}$ M; *c)* [**8**] = $3.1 \cdot 10^{-3}$ M and [**6c**] = $2.5 \cdot 10^{-5}$ M and [$C_6H_{10}Br_2$] = $1.2 \cdot 10^{-2}$ M; *d)* [**7b**] = $1.7 \cdot 10^{-5}$ M and [$C_6H_{10}Br_2$] = $1.1 \cdot 10^{-2}$ M. Solid lines: v = 20 mV/s; broken lines: v = 200 mV/s.

our measurements, we can conclude that these rates are similar for the subunits in **7b** and the 'free' **6c** and **8**, *i.e.* that Co^I is reformed by intramolecular electron transfer and that our concept of task-sharing in **7b** is effective. Completely reduced **7b** can be used as a sub-stoichiometric reducing agent in a molar ratio based on the electrons in the sponge as compared to those necessary per subtrate molecule transformation. An interesting question is still open. Can Co^I—V_5^0 perform reductions involving more than two electrons in a single elementary step – or more specific: Does the reduction of an aromatic nitro group or a 1,2,3,4,...-polyhalogenated substrate by **7b** as compared to an ordinary 'Co^I' catalyst without electron sponge lead to a different product distribution?

The authors thank PD Dr. *P. Bigler* and Dr. *Ch. Müller*, both from our institute, for extensive help in the structure elucidation of the corrin derivatives by NMR. Financial support by the *Swiss National Science Foundation* is gratefully acknowledged.

Experimental Part

1. *General.* Chemicals and solvents: *rac-trans*-1,2-dibromocyclohexane was prepared according to [28]. Hexane and MeCN from *Romil* (HPLC); pyridine (*Siegfried, purum*) was distilled from KOH; Et_2O (*Siegfried, PHHVI*) was distilled from NaH; HCl (37%, *Siegfried, purum*); $NaHCO_3$ (*Siegfried PHHVI*); CH_2Cl_2 (*Thommen, purum*) was distilled from P_2O_5 and filtered through aluminium oxide (*Camag*, B.-Akt. I). All other reagents and solvents from *Fluka*: MeOH, butan-2-one, benzene (stored over molecular sieve 4 Å), 1-methyl-1*H*-pyrrolidin-2-one (NMP), DMF (distilled from P_2O_5), $HClO_4$ (70%), $NaClO_4 \cdot H_2O$, NaI (dried at 100°/high vacuum, 12 h), NaOAc (H_2O-free), and KCN *puriss. p.a.*; MsCl *puriss.*; tetrabutylammonium perchlorate ($(Bu_4N)ClO_4$) *puriss.*, electrochemical grade; AcOMe (stored over molecular sieve 4 Å), butan-2-ol, hexamethylphosphoramide (HMPA; distilled before use), $NaBH_4$, and CF_3CO_2H (distilled before use) *purum* grade; $CHCl_3$ (UV-spectroscopy grade) was filtered through aluminium oxide before use. TLC: plates coated with silica gel *60* F_{254} (*Merck* Art. 5715), silica gel *RP-8* F_{254s} (*Merck* Art. 15388), or cellulose *F* (*Merck* Art. 5718). Column chromatography (CC): silica gel *60* $PF_{254+366}$ (for prep. TLC; *Merck* Art. 7748) or *Amberlite XAD-2* (*Servachrom*, 'reinst', 20–50 µm). HPLC: *Altex-100* solvent-metering pump with prep. head; flow rate 0–28 ml/min; *Uvikon 720 LC* UV/VIS detector; *LiChrosorb RP-8* (*Merck*), 7 µm, 23 mm × 250 mm. UV/VIS: *Hewlett-Packard 8451A* diode array spectrophotometer. CD: *JASCO Model 1 J-500A*; citation of λ_{max} (log $\Delta\varepsilon$) and zero passages λ_0 in nm. IR: *Perkin-Elmer 782*. ^1H-NMR: *Bruker AM-400WB* (400 MHz); TMS ($CDCl_3$, CD_3OD) or DSS (2,2-dimethyl-2-silapentane-5-sulfonate; D_2O) as internal reference, chemical shifts in ppm with δ (TMS) = 0 or δ (DSS) = 0; coupling constants *J* in Hz. ^{13}C-NMR: *Bruker AM-400WB* (100 MHz); TMS ($CDCl_3$, CD_3OD) or DSS (D_2O) as internal reference, chemical shifts in ppm with δ (TMS) = 0 or δ (DSS) = 0; multiplicities from the DEPT spectrum. Fast atom bombardment(FAB)-MS: *VG ZAB 2F*; saddle field atom gun; Xe bombardment (5 kV, 0.1 mA); 3-(benzyloxy)propane-1,2-diol(PDBE) matrix.

2. *Electrochemistry.* 2.1. As potentiostat, either a *Pine Instrument Company AFRDE 3* or an *EG & G P.A.R. model 173/179* with function generator *175* from *Princeton Applied Research* was used.

2.2. *Spectroelectrochemistry.* See *Fig. 8*.

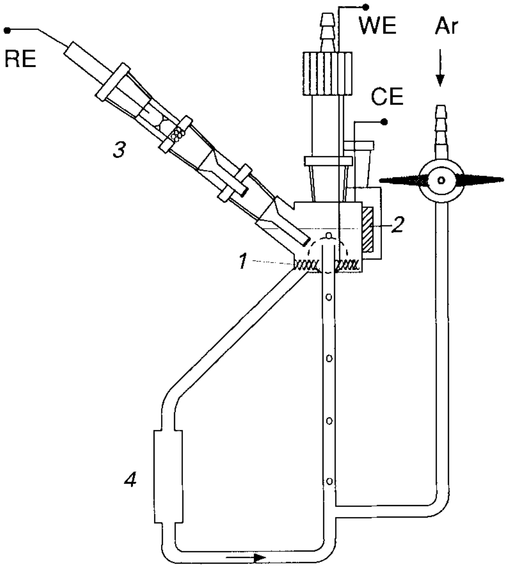

Fig. 8. *H-Type spectroelectrochemical bulk electrolysis cell. 1*) Working electrode (We, carbon felt (*Sigratherm, felt GFA 5, Sigri Elektrodengraphit GmbH*, D-8901 Meitingen), Pt-wire contacted) in electrolysis compartment. Forced circulation of the electrolyte solution (25 ml) through the cuvette *via* glass tubings (diam. 3 mm) by regulated Ar flushing. *2*) Counter electrode (CE, Pt-foil) in a compartment (volume 5 ml) separated from *1*). by a *P4* glass frit. *3*) Reference electrode (RE, SCE) doubly separated by ceramic diaphragms. *4*) Quartz cuvette (*d* = 2 mm). Electrochemical efficiency: $t_{1/2} \approx 2$ to 3 min. Mixing efficiency: *ca.* 2 s for 0.1-ml addition. The whole arrangement is installed in the spectrophotometer.

2.3. *Cyclic and Linear Sweep Voltammetry.* All measurements were performed in *Metrohm* cells under Ar at 22 ± 2°. The working electrode was a *Metrohm* (*6.2803.000*) glassy carbon electrode (3 mm active diameter). The reference was a *Metrohm* (*6.0804.100*) KCl-sat. aq. calomel electrode (SCE), separated from the soln. by a salt bridge containing the same solvent and electrolyte as the soln. The counter electrode was a Pt-wire placed directly in the soln.

3. *Rate Measurements of* trans-*1,2-Dibromocyclohexane* ($C_6H_{10}Br_2$) *Reduction.* 3.1. $k_1(V^+)$ *by Time-Resolved VIS Spectroscopy.* In a typical measurement, a soln. of **8** ($5 \cdot 10^{-5}$ M) in DMF/(Bu_4N)ClO_4 (15 ml, 0.1M) was completely reduced to V^+ at −650 mV *vs.* SCE in the spectroelectrochemical cell under Ar-forced convection at r.t. The potentiostat was then switched off, and O_2-free $C_6H_{10}Br_2$ (0.5 ml, $3.7 \cdot 10^{-3}$ mol, 0.24M) was added by syringe. The disappearance of the absorbance of V^+ ($\lambda = 610$ nm) was monitored every 20 s for 480 s, *i.e.* for several half-lives of V^+. The slope of the linear plot of ln(abs) *vs.* time ($-3.88 \cdot 10^{-3} s^{-1}$, correl. = 0.998) yielded the observed pseudo-1st-order rate constant which after correction for [$C_6H_{10}Br_2$] and a factor of 2 for the stoichiometry translated into $k_1 = 8 \cdot 10^{-3}$ l/mol·s.

3.2. $k_1(V^0)$. 3.2.1. *By CV.* In a typical series of measurements, the influence of the [$C_6H_{10}Br_2$] (from 30 to $900 \cdot 10^{-3}$ M) on the CV response of **8** ([V^{++}] = $4.5–3.9 \cdot 10^{-3}$ M) in DMF/(Bu_4N)ClO_4 (5 ml, 0.1M) was studied in the potential range 0 to −1V at r.t. and $v = 20$ to 100 mV/s. Increased cathodic (i_{pc}(cat)) and reduced anodic peak currents on the V^+/V^0 wave were observed in presence of $C_6H_{10}Br_2$ as compared to the situation in absence of $C_6H_{10}Br_2$ (i_{pc}(dif)). (No catalysis on the V^{++}/V^+ wave was observed even at high [$C_6H_{10}Br_2$].) From the current ratio i_{pc}(dif)/i_{pc}(cat), the observed pseudo-1st-order rate constant was determined according to [21b]. After correction for [$C_6H_{10}Br_2$], $k_1(V^0) = 1.0 \pm 0.5$ l/mol·s was obtained.

3.2.2. *By Time-Resolved VIS Spectroscopy.* Generally the same method as described for $k_1(V^+)$ was used, but the reduction was carried out at −1 V *vs.* SCE and lower [$C_6H_{10}Br_2$] (*e.g.* $30 \cdot 10^{-3}$ M) as well as shorter intervals for the absorbance measurements were used (*e.g.* every 0.5 s during 20 s) to monitor the formation of V^+ at 610 nm. Slopes of the ln(abs) *vs.* time were slightly curved (corr. = 0.98) and yielded, after the same corrections as described above, $k_1(V^0) = 1 \pm 0.8$ l/mol·s.

3.3. $k_1(Co^I)$ *by LSV.* In a typical series of measurements, the influence of [$C_6H_{10}Br_2$] (1 to $6 \cdot 10^{-3}$ M) in DMF/(Bu_4N)ClO_4 (5 ml, 0.1M) on the cathodic current response of **6c** (5 to $7 \cdot 10^{-5}$ M) was studied in the potential range 0 to −1.1 V at r.t. Plateau currents were observed on the Co^{II}/Co^I reduction wave and analyzed according to [21] yielding $k_1 = 4.1 \cdot 10^4$ l/mol·s.

3.4. *Multiple Reductive Elimination of $C_6H_{10}Br_2$ by Completely Reduced* **7b** ($Co^I–V_5^0$). A soln. of **7b** (*ca.* 3.5 mg, $1.1 \cdot 10^{-6}$ mol, 0.07 mM) in 15 ml DMF/(Bu_4N)ClO_4 0.1M was reduced to $Co^I–V_5^0$ in the spectroelectrochemical cell. Upon addition of 100 equiv. of $C_6H_{10}Br_2$ instantaneous oxidation to $Co^{II}–V^{++}$ was observed. GC analysis of the mixture (*OV-1701 vi* on 30 m *Duran* glass, diameter 0.5 mm; temp. 60–155°, 3°/min; He) and comparison with authentic material revealed the formation of cyclohexene.

4. *Syntheses.* 4.1. Co*α*,Co*β-Dicyano[2,7,18-tris(2-hydroxyethyl)-3,8,13,17-tetrakis(3-hydroxypropyl)-1,2,5,7,12,12,15,17-octamethylcorrinato]cobalt(III)* (**2**). Heptamethyl *Co*-aqua-*Co*-cyanocoh(III)yrinate perchlorate (**1b**; 1.063 g, 0.9 mmol) was transformed into crude **2** according to [9]. Compound **2** was purified either by CC (200 g *XAD*, 4.5 × 17 cm, MeOH/H_2O (+0,1% (*v*/*v*) HCN) 1:1, 165 ml/h) or HPLC (silica gel *RP-8* (7 µm), 2.3 × 25 cm, MeOH/H_2O (+1% (*v*/*v*) HCN) 1:1 10 ml/h, 212.6 mg of product in 1.6 ml of soln. per charge). The front-fraction yielded, after evaporation at 40° and drying (high vacuum, r.t., 48 h), 591 mg (73%) and 611 mg (76%), resp., of **2**. Violet powder. TLC (silica gel *RP-8*, H_2O (+1% (*v*/*v*) HCN)/MeOH 1:1): R_f 0.34. UV/VIS (MeOH (+0.1% (*v*/*v*) HCN), $c = 3.39 \cdot 10^{-5}$ M): 278 (3.98), 312 (3.91), 353 (sh, 4.11), 368 (4.43), 418 (3.37), 510 (sh, 3.91), 540 (3.90), 578 (3.98). CD (MeOH (+0.1% (*v*/*v*) HCN), $c = 3.39 \cdot 10^{-5}$ M): 284 (0.89), 306 (−8.26), 317 (−3.68), 322 (−5.36), 327 (−5.25), 345 (−10.05), 358 (−5.25), 363 (−6.03), 393 (15.29), 413 (10.49), 421 (11.16), 515 (−1.78), 533 (−2.68), 552 (−1.79), 577 (−3.68); λ_0 = 277, 288, 371, 459, 605. IR (KBr): a.o. 3400*s* (br.), 2950*m*, 2880*m*, 2120*w*, 1625*m*, 1585*s*, 1505*s*, 1405*s*, 1365*s*, 1355*m*, 1225*m*, 1200*m*, 1150*s*, 1115*s*, 1055*s*. ^{1}H-NMR (400 MHz, CD_3OD): 1.18, 1.31, 1.40, 1.41, 1.47, 1.56, 2.28, 2.32 (8 *s*, 8 Me) superimposed by 1.15–2.35 (*m*, 22 H); 2.63 (*dt*-like, $J \approx 2(d)$, $J \approx 10(t)$, H–C(18)); 3.01–3.11 (*m*, H–C(8), H–C(13)); 3.40–3.90 (*m*, 7 CH_2O, H–C(3)); 3.91 (*d*, $J = 10.5$, H–C(19)); 4.89 (*s*, H_2O); 5.67 (*s*, H–C(10)). ^{13}C-NMR (100 MHz, CD_3OD): 15.89, 16.09, 17.33, 18.53, 19.96, 21,13, 23.04 (7*q*, *C*H_3–C(1), *C*H_3–C(2), *C*H_3–C(5), *C*H_3–C(7), α-*C*H_3–C(12), *C*H_3–C(15), *C*H_3–C(17)); 27.31, 28.06, 29.13, 29.35, 30.65, 30.78 (6*t*, 6 CH_2); 31.55 (*q*, β-*C*H_3–C(12)); 31.89, 34.48, 36.46 (3*t*, 3 CH_2); 40.45 (*d*, C(18)); 40.52, 44.18 (2*t*, 2 CH_2); 47.42, 47.93, 49.89 (3*s*, C(2), C(7), C(12)); 55.62, 57.96, 59.17 (3*d*, C(3), C(8), C(13)); 59.36 (*s*, C(17)); 59.59, 59.92, 60.73 (3*t*, C(2^2), C(7^2), C(18^2)); 62.57, 62.86, 63.09, 63.18 (4*t*, C(3^3), C(8^3), C(13^3), C(17^3)); 77.35 (*d*, C(19)); 84.39 (*s*, C(1)); 91.18 (*d*, C(10)); 103.58, 104.96 (2*s*, C(5), C(15));

135.20, 135.76 (2*s*, 2 CN); 164.82, 165.61 (2*s*, C(6), C(14)); 174.43 (*s*, C(9)); 177.82, 177.89, 178.74 (3*s*, C(4), C(11), C(16)). FAB-MS (PDBE): 892 (8, M^{+}), *865* (100, $[M - \text{HCN}]^{+}$), 839 (94, $[M - \text{HCN} - \text{CN}]^{+}$), 793, (26).

4.2. Coα,Coβ*-Dicyano{2,7,18-tris[2-(methylsulfonyloxy)ethyl]-3,8,13,17-tetrakis[3-(methylsulfonyloxy)propyl]-1,2,5,7,12,12,15,17-octamethylcorrinato}cobalt(III)* (**3**; modification of a known procedure [13]). To a stirred soln. of **2** (591 mg, 0.66 mmol) in pyridine (60 ml) under Ar at –15°, MsCl (0.45 ml, 5.8 mmol) was added within 5 min. Stirring was continued at 2° for 4 h and the mixture poured in 37% aq. HCl soln. (62 ml)/ice (62 g) and extracted with ice-cooled CH_2Cl_2 (1 × 130 ml, 1 × 50 ml). The combined org. phase was washed successively with ice-cooled soln. of 1M HCl (70 ml), 0.05M $NaHCO_3$ (until pH neutral), aq. HCN soln. (0.5% (*v*/*v*), 70 ml), and H_2O (70 ml), filtered through cotton, and evaporated at 30°, and the crude product was purified by CC (60 g of silica gel, 4 × 11.5 cm, CH_2Cl_2/MeOH 98:2 (+0.05% (*v*/*v*) HCN), 1 ml/2 min; column packing with CH_2Cl_2/MeOH 99:1 (+0.05% (*v*/*v*) HCN)). The product fraction was evaporated at 30°, the residue dissolved in CH_2Cl_2, the soln. filtered through a *P4* glass frit and evaporated at r.t., and the residue dried at r.t./high vacuum for 12 h: 828 mg (86%) of **3**. Violet powder. TLC (CH_2Cl_2/MeOH (+1% (*v*/*v*) HCN) 97:3): R_f 0.23. UV/VIS (CH_2Cl_2, $c = 3.33 \cdot 10^{-5}$ M): 280 (4.09), 316 (4.01), 356 (sh, 4.15), 372 (4.51), 422 (3.49), 513 (sh, 3.76), 548 (3.99), 588 (4.08). CD (CH_2Cl_2, $c = 3.33 \cdot 10^{-5}$ M): 281 (1.48), 310 (–10.57), 320 (–5.23), 327 (–9.09), 330 (–8.75), 348 (–14.43), 359 (–8.18), 367 (–12.95), 394 (21.82), 418 (12.95), 425 (14.09), 522 (–0.57), 539 (–1.36), 561 (–0.57), 585 (–3.29); λ_0 = 273, 289, 374, 460, 606. IR ($CHCl_3$): a.o. 3020*m*, 2990*m*, 2970*m*, 2940*m*, 2110*w*, 1580*s*, 1505*s*, 1470*m*, 1450, 1400*s*, 1355*s*, 1175*s*, 1150*s*, 1135*m*, 1115*s*, 1030*m*, 970*s*, 955*s*, 925*s*, 820*m*, 503*s*. ^{1}H-NMR (400 MHz, $CDCl_3$): 1.57, 1.49, 1.41, 1.38, 1.33, 1.22 (6*s*, 6 Me); 2.22, 2.26 (2*s*, Me–C(5), Me–C(15)), superimposed by 1.60–3.37 (*m*, 22 H); 2.59 (*t*-like, $J \approx 10$, H–C(18)); 2.93–3.07 (*m*, superimposed by 2.93, 2.97, 2.98, 3.04, 3.05, 3.06 (6*s*, 6 $MeSO_3$), total 20 H); 3.09 (*s*, $MeSO_3$); 3.15 (*d*-like, $J \approx 8$, 1 H); 3.92 (*d*, $J = 10$, H–C(19)); 4.10–4.70 (*m*, 7 CH_2O); 5.57 (*s*, H–C(10)). ^{13}C-NMR (100 MHz, $CDCl_3$): 15.43, 15.65 (2*q*, CH_3–C(15), CH_3–C(5)); 18.35, 18.39, 19.56, 21.46, 22.86 (5*q*, CH_3–C(1), CH_3–C(2), CH_3–C(7), α-CH_3–C(12), CH_3–C(17)); 25.01, 25.70, 25.91 (2 C), 26.21, 27.49, 28.00, 30.13, (7*t*, 8 CH_2); 31.52 (*q*, β-CH_3–C(12)); 34.97 (*t*, 1 CH_2); 37.17, 37.29 (2 C), 37.32, 37.58, 37.77, 37.86 (6*q*, 7 CH_3SO_3); 38.09 (*t*, 1 CH_2); 38.57 (*d*, C(18)); 41.09 (*t*, 1 CH_2); 46.42, 46.83 (2*s*, C(2), C(12)); 48.49 (*s*, C(7)); 53.97 (*s*, C(13)); 56.54 (*d*, C(8)); 57.90 (*d*, C(3)); 57.95 (*s*, C(17)); 67.31, 67.52, 67.61 (3*t*, C(2^2), C(7^2), C(18^2)); 69.26, 70.27, 70.44, 70.98 (4*t*, C(3^3), C(8^3), C(13^3), C(17^3)); 75.66 (*d*, C(19)); 82.69 (*s*, C(1)); 89.99 (*d*, C(10)); 102.43 (*s*, C(15)); 103.48 (*s*, C(5)); 130.42, 131.19 (2*s*, 2 CN); 162.87, 163.32 (2*s*, C(6), C(14)); 171.66 (*s*, C(9)); 174.96, 176.29, 176.99 (3*s*, C(4), C(11), C(16)). FAB-MS (PDBE): 1438 (7, M^{+}), 1411 (84, $[M - \text{HCN}]^{+}$), 1386 (95, $[M - 2\,\text{CN}]^{+}$), 1332 (32), *1306* (100), 1289 (45).

4.3. Coα,Coβ*-Dicyano[2,7,18-tris(2-iodoethyl)-3,8,13,17-tetrakis(3-iodopropyl)-1,2,5,7,12,12,15,17-octamethylcorrinato]cobalt(III)* (**4**). Compound **3** (505 mg, 0.35 mmol) was heated under reflux with dry NaI in butan-2-one (40 ml) under Ar for 15 min. The mixture was then quickly cooled to r.t., poured on H_2O (100 ml), and extracted with CH_2Cl_2 (100 ml). The org. phase was washed with aq. HCN soln. (100 ml, 0.5% (*v*/*v*)) and H_2O (100 ml), filtered through cotton, and evaporated at r.t. The residue was purified by CC (60 g of silica gel, 3 × 21 cm, CH_2Cl_2/MeOAc 94:6 (+0.1% (*v*/*v*) HCN, 23 ml/h) and the product fraction evaporated at r.t. The residue was dissolved in benzene, filtered through a *P4* glass frit, and precipitated upon addition to hexane. The solid was collected (*P4* glass frit), washed with hexane, and dried (high vacuum, r.t., 12 h): 449 mg (77%) of **4**. Violet powder. TLC (CH_2Cl_2/MeOAc 94:6 (+0.1% (*v*/*v*) HCN)): R_f 0.67. UV/VIS (MeOH (+0.05% (*v*/*v*) HCN), $c = 3.3 \cdot 10^{-5}$ M): 280 (4.07), 312 (3.98), 354 (sh, 4.16), 370 (4.49), 421 (sh, 3.43), 514 (sh, 3.72), 544 (3.95), 582 (4.04). CD (MeOH (+0.05% (*v*/*v*) HCN), $c = 3.3 \cdot 10^{-5}$ M): 253 (–19.69), 263 (–8.93), 279 (–20.15), 289 (–9.73), 309 (–21.18), 321 (–11.56), 324 (–11.79), 332 (–8.36), 346 (–11.68), 360 (–6.41), 367 (–8.13), 393 (17.97), 417 (10.99), 423 (11.56), 464 (1.14), 515 (3.66), 520 (3.32), 546 (5.72), 569 (4.35), 586 (5.49), 622 (0.46); λ_0 = 373. IR ($CHCl_3$): a.o. 2990*m*, 2125*m*, 1585*s*, 1500*s*, 1470*m*, 1450*m*, 1420*m*, 1400*m*, 1370*m*, 1355*m*, 1245*m*, 1155*s*, 1115*m*. ^{1}H-NMR (400 MHz, $CDCl_3$): 1.19, 1.31, 1.38 (6 H), 1.47, 1.50, 2.17, 2.29 (7*s*, 8 Me), superimposed by 1.40–2.48 (*m*, 22 H); 2.63 (*dt*-like, $J \approx 10$ (*t*), H–C(18)); 2.87 (*t*-like, $J \approx 6$, 1 H); 2.93–3.01 (*m*, 2 H); 3.02–3.33 (*m*, 12 H); 3.34–3.43 (*m*, 1 H); 3.59–3.68 (*m*, 1 H); 3.82 (*d*, $J = 10$, H–C(19)); 5.48 (*s*, H–C(10)). ^{13}C-NMR (100 MHz, $CDCl_3$): 0.00, 0.69, 6.72, 7.64, 9.26, 9.41, 10.69 (7*t*, C(2^2), C(7^2), C(18^2), C(3^3), C(8^3), C(13^3), C(17^3)); 16.72, 17.27, 17.92, 19.53, 21.14, 21.94, 24.21 (7*q*, CH_3–C(1), CH_3–C(2), CH_3–C(5), CH_3–C(7), α-CH_3–C(12), CH_3–C(15), CH_3–C(17)); 28.65, 30.65, 31.13, 31.66, 32.37, 32.49, (6*t*, 6 CH_2); 32.74 (*q*, β-CH_3–C(12)); 33.55, 35.27, 42.09, 42.52 (4*t*, 4 CH_2); 43.51 (*d*, C(18)); 47.29 (*t*, 1 CH_2); 48.10, 49.81, 53.07 (3*s*, C(2), C(7), C(12)); 55.26, 56.16, 57.69 (3*d*, C(3), C(8), C(13)); 58.95 (*s*, C(17)); 76.37 (*d*, C(19)); 84.30 (*s*, C(1)); 90.83 (*d*, C(10)); 103.22, 104.12 (2*s*, C(5), C(15)); 130.43, 132.59 (2*s*, 2 CN); 164.09, 164.56 (2*s*, C(6), C(14)); 172.61 (*s*, C(9)); 175.46, 177.16, 177.81 (3*s*, C(4), C(11), C(16)). FAB-MS (glycerol/thioglycerol): 1608 $[M - 2\,\text{HCN}]^{+}$, 1481 $[M - 2\,\text{HCN} - \text{I}]^{+}$, 1354, 1227, 1100, 973.

4.4. Coα,Coβ*-Dicyano[8^2,8^3-dihydro-2,7,18-tris(2-iodoethyl)-3,13,17-tris(3-iodopropyl)-1,2,5,7,12,12,15,17-octamethyl-8^1*H*-benzo[*hi*]corrinato]cobalt(III)* (**5a**). Compound **4** (805 mg, 0.56 mmol) was heated under reflux with dry NaI in butan-2-one (60 ml) under Ar for 8 h. The mixture was poured on H_2O (150 ml) and extracted with CH_2Cl_2 (1 × 150 ml). The org. phase was washed with aq. HCN soln. (100 ml, 0.5% (*v*/*v*)) and H_2O (100 ml), filtered through cotton, and evaporated at r.t. The residue was purified by CC (95 g of silica gel, 4 × 19 cm, CH_2Cl_2/MeOAc 94:6, 40 ml/h). The dark blue product fraction was evaporated at r.t. The residue was again dissolved in benzene, filtered through a *P4* glass frit, and precipitated upon addition to hexane. The solid was collected (*P4* glass frit), washed with hexane, and dried (high vacuum, r.t., 12 h): 732 mg (85%) of **5a**. Dark blue powder. TLC ($CHCl_2$/MeOAc 94:6 (+0.1% (*v*/*v*) HCN)): R_f 0.52. UV/VIS (MeOH (+0.05% (*v*/*v*) HCN), $c = 3.58 \cdot 10^{-5}$ M): 290 (4.02), 312 (3.96), 322 (3.95), 3.61 (sh, 4.14), 378 (4.45), 432 (sh, 3.23), 535 (sh, 3.66), 572 (3.93), 612 (4.11). CD (MeOH (+0.05% (*v*/*v*) HCN), $c = 3.58 \cdot 10^{-5}$ M): 254 (−21.98), 265 (−12.89), 289 (−39.31), 302 (−23.67), 307 (−25.79), 316 (−20.08), 319 (−20.50), 334 (−2.75), 343 (−4.44), 360 (sh, 4.65), 376 (33.82), 390 (sh, 19.23), 405 (sh, 15.64), 445 (2.96), 485 (5.92), 577 (−4.86), 588 (−4.44), 615 (−8.24); λ_0 = 352, 550, 651. IR ($CHCl_3$): a.o. 2980*m*, 2950*m* (sh), 2880*w*, 2120*w*, 1615*w*, 1560*m*, 1500*s*, 1455*m*, 1445*m*, 1430*m*, 1390*w*, 1380*w*, 1340*m*, 1245*m*, 1160*m*, 1145*m*, 1125*m*, 1090*s*, 1055*w*, 1040*w*. ^{1}H-NMR (400 MHz, $CDCl_3$): 1.15, 1.26, 1.28, 1.38, 1.50 (6 H), 2.20, 2.26 (7*s*, 8 Me), superimposed by 1.41–2.37 (*m*, 22 H); 2.58–2.79 (*m*, 4 H); 2.82–2.90 (*m*, 2 H); 2.99–3.33 (*m*, 10 H); 3.34–3.42 (*m*, 1 H); 3.58–3.65 (*m*, 1 H); 3.69 (*d*, *J* = 10, H–C(19)). ^{13}C-NMR (100 MHz, $CDCl_3$): 0.00, 1.36, 6.85, 8.12, 9.11, 10.10 (6*t*, C(2^2), C(7^2), C(18^2), C(3^3), C(13^3), C(17^3)); 16.02, 18.17, 18.41, 20.71, 23.27, 24.39, 24.92 (7*q*, CH_3–C(1), CH_3–C(2), CH_3–C(5), CH_3–C(7), α-CH_3–C(12), CH_3–C(15), CH_3–C(17)); 22.51, 24.52, 27.81, 29.58 (4*t*, 4 CH_2); 30.27 (*q*, β-CH_3–C(12)); 32.14, 33.11, 33.18, 34.12, 36.06, 42.25, 43.02 (7*t*, 7 CH_2); 44.06 (*d*, C(18)); 44.69 (*t*, 1 CH_2); 50.39, 51.13, 53.43, (3*s*, C(2), C(7), C(12)); 53.26, 58.07, 58.37 (3*d*, C(3), C(8), C(13)); 59.72 (*s*, C(17)); 77.78 (*d*, C(19)); 84.22 (*s*, C(1)); 103.13, 103.59, 104.75 (3*s*, C(5), C(10), C(15)); 132.38, 134.23 (2*s*, 2 CN); 162.67, 165.94, (2*s*, C(6), C(14)); 170.01 (*s*, C(9)); 174.34, 175.33, 176.49 (3*s*, C(4), C(11), C(16)). FAB-MS (PDBE): 1534 (9, $M^{+\cdot}$), *1507* (100, $[M - \mathrm{HCN}]^+$), 1480 (65, $[M - 2\,\mathrm{HCN}]^+$), 1405 (34), 1379 (63), 1353 (80, $[M - 2\,\mathrm{CN} - \mathrm{I}]^+$).

4.5. *Coβ(or Coα)-Cyano[8^2,8^3-dihydro-2,7,18-tris(2-iodoethyl)-3,13,17-tris(3-iodopropyl)-1,2,5,7,12,12,15,17-octamethyl-8^1*H*-benzo[*hi*]corrinato]-*Coα (or Coβ)*-iodocobalt(III)* (**5b**). To a soln. of **5a** (511 mg, 0.33 mmol) in $CHCl_3$ (100 ml), CF_3CO_2H (0.15 ml, 1.96 mmol) was added (color change from dark blue to red) and stirred at r.t. for 15 min under Ar. *Ca.* 50 ml of the solvent were evaporated at r.t. After addition of $CHCl_3$ (50 ml), the mixture was stirred at r.t. under Ar for additional 5 min. This procedure was repeated once (to remove HCN). The mixture was diluted with CH_2Cl_2 (100 ml) and washed twice with aq. phosphate buffer (1M, pH 3, 100 ml) containing KI (1.18 g, color change to very dark blue). The org. phase was filtered through cotton and evaporated and the residue purified by CC (30 g of silica gel containing NaI (3 g), 3 × 9.5 cm, CH_2Cl_2/AcOMe 94:6, 22 ml/h). The solvent of the dark blue product fraction was evaporated at r.t. The residue was dissolved in benzene, filtered through a *P4* glass frit, precipitated upon addition to hexane, and collected (*P4* glass frit). The product was washed with hexane and dried (high vacuum, r.t., 12 h): 482 mg (89%) of **5b**. Dark blue powder. TLC[8] (CH_2Cl_2/AcOMe 94:6 (+0.1% (*v*/*v*) HCN), blue spot): R_f 0.52. UV/VIS (benzene, rel. int.): 316 (sh, 0.86), 327 (sh, 0.79), 390 (1), 440 (sh, 0.19), 589 (sh, 0.45), 620 (0.52). IR ($CHCl_3$): a.o. 2970*s*, 2870*m*, 2150*w*, 2130*w*, 1610*m*, 1555*s*, 1540*m*, 1495*m*, 1455*m*, 1440*m*, 1430*m*, 1390*m*, 1380*m*, 1335*m*, 1320*m*, 1240*m*, 1145*m*, 1125*m*, 1095*s*. ^{1}H-NMR (400 MHz, $CDCl_3$): 1.13, 1.21, 1.42, 1.43, 1.71, 2.25, 2.33 (8*s*, 8 Me), superimposed by 1.60–2.40 (*m*, 20 H); 2.50–2.60 (*m*, 1 H); 2.65–2.96 (*m*, 4 H); 2.98–3.44 (*m*, 14 H); 3.57–3.65 (*m*, 1 H); 4.36 (*d*, *J* = 10, H–C(19)). FAB-MS (glycerol/thioglycerol): 1480 (92, $[M - \mathrm{HCN} - \mathrm{HI}]^+$), *1353* (100, $[M - \mathrm{HI} - \mathrm{I}]^+$), 1226 (61), 1100 (62), 973 (30).

4.6. *Coα,Coβ-Dicyano[8^2,8^3-dihydro-2,7,18-tris(2-acetoxyethyl)-3,13,17-tris(3-acetoxypropyl)-1,2,5,7,12,12,15,17-octamethyl-8^1*H*-benzo[*hi*]corrinato]cobalt(III)* (**6a**). A soln. of **5a** (395 mg, 0.257 mmol) and NaOAc (1.25 g, 15.2 mmol) in HMPA (36 ml) was stirred at r.t. under Ar for 3 h. The mixture was poured on ice-cooled CH_2Cl_2/H_2O 1:2 (150 ml). The org. phase was washed with H_2O (10 × 100 ml) and with 0.5% (*v*/*v*) aq. HCN soln. (15 × 50 ml), filtered through cotton, and evaporated. HMPA was removed from the oily residue by CC (45 g of silica gel, 3 × 15 cm, CH_2Cl_2/MeOH 97:3 (+0.1% (*v*/*v*) HCN), 34 ml/h; column packing with CH_2Cl_2/MeOH 98:2 (+0.1% (*v*/*v*) HCN). The combined product fractions yielded a mixture of products which was further purified by CC (13 g of silica gel, 2 × 10 cm, CH_2Cl_2/MeOH 98:2 (+0.1% (*v*/*v*) HCN), 17 ml/h). The product fraction was evaporated, again dissolved in benzene, filtered through a *P4* glass frit, precipitated upon addition to hexane, and collected (*P4* glass frit) to yield, after drying (high vacuum, r.t., 12 h), 192 mg (66%) of **6a**. Dark blue powder. TLC (CH_2Cl_2/MeOH (+1% (*v*/*v*) HCN) 96:4): R_f 0.41. UV/VIS (MeOH (+0.1% (*v*/*v*) HCN), $c = 3.58 \cdot 10^{-5}$ M): 290 (4.01, 310 (3.96), 320 (3.96), 360 (sh, 4.17), 376 (4.48), 420 (sh, 3.39), 533 (sh, 3.71), 570 (3.96), 608 (4.12). CD (MeOH (+0.1% (*v*/*v*) HCN), $c = 3.58 \cdot 10^{-5}$ M): 253 (−18.81), 263 (−10.36), 287 (−20.59), 300 (−19.66), 306

---

[8] During TLC, the corresponding [$Co^{III}(CN)_2$(corrinato)] complex was formed.

(−21.14), 317 (sh, −15.43), 332 (−2.11), 341 (−4.65), 360 (sh, 6.34), 374 (27.83), 388 (sh, 22.19), 404 (sh, 17.75), 443 (2.54), 4.75 (4.86), 575 (−11.41), 581 (−10.99), 609 (−17.54); $\lambda_0 = 350, 525, 675$. IR ($CHCl_3$): a.o. 2980*s*, 2880*m*, 2120*w*, 1735*s*, 1615*m*, 1560*m*, 1540*m*, 1500*s*, 1480*m*, 1470*m*, 1455*m*, 1445*m*, 1430*m*, 1390*s*, 1370*s*, 1340*m*, 1310*m*, 1240*s*, 1175*m*, 1105*m*, 1115*s*, 1105*s*, 1085*s*, 1035*s*. ^{1}H-NMR (400 MHz, $CDCl_3$): 1.15 (*s*, Me–C(7)); 1.271 (*s*, β-Me–C(12)); 1.274 (*s*, Me–C(17)); 1.29 (*s*, Me–C(12)); 1.44 (*s*, Me–C(1)); 1.50 (*s*, α-Me–C(12)); 1.83 (*s*, H_2O); superimposed by 1.45 (H–C(8^1)), 1.46 (H–C(3^1)), 1.52 (H–C(13^1)), 1.54 (H–C(17^2)), 1.60 (H–C(17^3)), 1.69 (H–C(13^2)), 1.71 (H–C(2^1)), 1.73 (H–C(8^2)), 1.78 (H′–C(13^1), H′–C(13^2)), 1.86 (CH_2(3^2)), 1.84 (H′–C(2^1)), 1.85 (H′–C(8^1)), 1.87 (H′–C(17^2), total 15 H); 2.01, 2.03, 2.05, 2.08, 2.09, 2.12 (6*s*, 6 OCOMe); 2.21 (*s*, Me–C(5)); 2.22 (*s*, Me–C(15)); superimposed by 2.02 (H–C(7^1)), 2.04 (H′–C(3^1), CH_2(18^1)), 2.06 (H′–C(8^2)), 2.16 (H′–C(17^1), total 6 H); 2.37 (*m*, H′–C(7^1)); 2.53 (*dt*-like, $J \approx 10$ (*t*), H–C(18)); 2.62 (*m*, H–C(8^3)); 2.76 (*m*, H′–C(8^3)); 2.84 (*dd*, $J = 7, 5$, H–C(13)); 2.98 (*d*-like, H–C(8)); 3.00 (*d*-like, H–C(3)); 3.82 (*d*, $J = 9.8$, H–C(19)); 4.04 (*m*, CH_2(13^3)); 4.11 (*m*, CH_2(3^3), CH_2(17^3)); 4.11, 4.19 (*m*, CH_2(7^2), 4.19 (*m*, CH_2(2^2), H–C(18^2)); 4.30 (*m*, H′–C(18^2)). ^{13}C-NMR (100 MHz, $CDCl_3$): 14.50 (*q*, CH_3–C(5)); 16.12 (*q*, CH_3–C(15)); 16.18 (*q*, CH_3–C(2)); 19.42 (*q*, CH_3–C(17)); 20.86, 20.89, 21.02, (3 C) (4*q*, 6 CH_3COO); 20.91 (*t*, C(8^1)); 21.82 (*q*, CH_3–C(7)); 22.61 (*q*, α-CH_3–C(12)); 22.68 (*q*, CH_3–C(1)); 22.74 (*t*, C(8^2)); 24.71 (*t*, C(17^2)); 26.01 (*t*, C(8^3)); 26.06 (*t*, C(3^1)); 26.96 (*t*, C(18^1)); 26.99 (*t*, C(13^2)); 27.91 (*t*, C(13^1)); 28.62 (*q*, β-CH_3–C(12)); 30.04 (*t*, C(3^2)); 34.63 (*t*, C(2^1)); 35.99 (*t*, C(17^1)); 36.54 (*t*, C(7^1)); 39.09 (*d*, C(18)); 46.50 (*s*, C(2)); 47.84 (*s*, C(7)); 48.69 (*s*, C(12)); 52.51 (*d*, C(8)); 56.97 (*d*, C(13)); 58.29 (*d*, C(3)); 58.32 (*s*, C(17)); 61.31 (*t*, C(2^2)); 61.50 (*t*, C(7^2)); 62.15 (*t*, C(18^2)); 63.79, 63.99 (2*t*, C(3^3), C(17^3)); 64.67 (*t*, C(13^3)); 76.52 (*d*, C(19)); 82.25 (*s*, C(1)); 101.61, 101.67 (2*s*, C(5), C(10)); 102.63 (*s*, C(15)); 130.78, 132.47 (2*s*, 2 CN); 161.65 (*s*; C(6)); 164.27 (*s*, C(14)); 168.71 (*s*, C(9)); 170.67, 170.84, 170.97, 170.99, 171.03, 171.06 (6*s*, 6 CH_3CO); 173.17 (*s*, C(4)); 173.34 (*s*, C(11)); 174.91 (*s*, C(16)). FAB-MS (PDBE): 1126 (42, $M^{+\cdot}$), 1099 (100, $[M - HCN]^+$), 1074 (64, $[M - 2\,CN]^+$), 1013 (16), 985 (10).

4.7. Coα(or Coβ)-*Aqua*-Coβ(or Coα)-*cyano[8²,8³-dihydro-2,7,18-tris(2-acetoxyethyl)-3,13,17-tris(3-acetoxypropyl)-1,2,5,7,12,12,15,17-octamethyl-8¹*H-*benzo[*hi*]corrinato]cobalt(III) Perchlorate* (**6b**). To a soln. of 55 mg (0.048 mmol) of **6a** in 20 ml of $CHCl_2$, 20 µl (0.26 mmol) of CF_3CO_2H were added under Ar at r.t. (color changes from blue to red). After 15 min, 10 ml of the solvent were evaporated and replaced by fresh $CHCl_3$, and the soln. was stirred again for 5 min. This procedure was repeated once. The mixture was then diluted with CH_2Cl_2 (20 ml), washed twice with 40 ml of 1M phosphate buffer (pH 3) containing $NaClO_4$ (0.4 g), and filtered through cotton. After solvent evaporation and drying (high vacuum, r.t., 12 h) 59 mg (98%) of **6b** were obtained. Red varnish. TLC[8]) (CH_2Cl_2/MeOH (+1% (*v*/*v*) HCN) 96:4, blue spot): R_f 0.41. UV/VIS (MeOH, rel. int.): 286 (0.39), 328 (0.55), 360 (1.0), 410 (sh, 0.19), 510 (0.34), 540 (0.37). UV/VIS (MeOH/H_2O 1:1, rel. int.): 288 (0.38), 328 (0.49), 362 (1.0), 410 (sh, 0.17), 518 (sh, 0.33), 544 (0.37). IR (KBr): a.o. 3720–3100*m* (br.), 2965*m*, 2870*w*, 2130*w*, 1740*s*, 1615*w*, 1560*m*, 1500*s*, 1390*m*, 1370*s*, 1240*s*, 1150*m*, 1120*s*, 1110*s*, 1090*s*, 1035*s*.

4.8. *[8²,8³-Dihydro-2,7,18-tris(2-acetoxyethyl)-3,13,17-tris(3-acetoxypropyl)-1,2,5,7,12,12,15,17-octamethyl-8¹*H-*benzo[*hi*]corrinato]perchloratocobalt(II)* (**6c**). To 57 mg (0.047 mmol) of **6b** in 15 ml MeOH/H_2O 1:1 in a separating funnel, a layer of 70 ml of Et_2O/hexane 1:1 was added. The two-phase system was bubbled with Ar for 30 min. Then 0.3 g (7.9 mmol) of $NaBH_4$ were added, and the whole system was thoroughly shaken (H_2 evolution!). The blue H_2O phase was discarded, the dark green org. phase washed with 30% aq. $HClO_4$ soln. (7 ml) and H_2O (10 ml), and the combined, brown aq. phase extracted with CH_2Cl_2 (1 × 40 ml, 1 × 10 ml). The combined org. phases were washed with 40 ml of 0.1M phosphate buffer (pH 4) containing $NaClO_4$ (0.4 g), filtered through cotton, and evaporated. After drying (high vacuum, r.t., 12 h), 39.7 mg (72%) of **6b** were obtained. Dark brown varnish. TLC[8]) (CH_2Cl_2/MeOH (+1% (*v*/*v*) HCN) 96:4, blue spot): R_f 0.41. UV/VIS (CH_2Cl_2, rel. int.): 274 (0.84), 316 (1.0), 408 (0.35), 486 (0.42). IR (KBr): a.o. 2970*m*, 2870*w*, 1740*s*, 1500*m*, 1385*m*, 1370*m*, 1240*s*, 1145*m*, 1120*s*, 1110*s*, 1090*s*, 1035*m*.

4.9. Coα(or Coβ)-*Aqua*-Coβ(or Coα)-*cyano{2¹,2²,8²,8³-tetrahydro-7,18-bis[2-(1′-methyl-4,4′-bipyridinio)ethyl]-3,13,17-tris[3-(1′-methyl-4,4′-bipyridinio)propyl]-1,2,5,7,12,12,15,17-octamethyl-8¹*H-*benzo[*hi*]cyclopenta[*as*]corrinato}cobalt(III) Undecachloride* (**7a**). A soln. of **5b** (740 mg, 0.45 mmol) and 1-methyl-4,4′-bipyridinium iodide [14] in NMP (75 ml) was stirred at 80° under Ar for 24 h. After cooling to r.t., MeCN (250 ml) was added and a flocky solid precipitated. After filtration through a *P4* glass frit, further precipitation was achieved upon addition of Et_2O (100 ml) to the filtrate. The combined residue was again dissolved in NMP (26 ml), precipitated upon successive addition of MeCN (250 ml) and Et_2O (100 ml), collected (*P4* glass frit), and washed with MeCN/Et_2O 5:2 (50 ml). The red-brown solid was then dissolved in H_2O (10 ml) and ion exchanged on a Cl^--charged *Dowex 2* column (30 g *Dowex 2* (*Fluka*, *X 8*, 20–50 mesh), 1.5 × 35 cm, 1 drop/s). The red-violet varnish, obtained after evaporation of the eluate at 45°, was purified by CC (200 g *XAD*, 2.5 × 48 cm, H_2O, 30 ml/h). After evaporation of the red-violet main fraction at 45°, the residue was dried (high vacuum, r.t., 12 h): 483 mg (49%, corrected for 8% H_2O content) of **7a**. TLC[8]) (cellulose, butan-2-ol sat. with H_2O (+0.1% (*v*/*v*) HCN), blue spot): R_f 0.06. UV/VIS (dist. H_2O (+ trace KCN), rel. int.): 204 (1), 264 (0.99), 318 (sh, 0.074), 336 (sh, 0.039), 360 (sh, 0.10), 378 (0.20), 403 (sh, 0.069), 535 (sh, 0.033), 570 (0.056), 608 (0.081). UV/VIS (MeOH/dist. H_2O 1:1, rel. int.): 262 (1), 328 (0.082), 366 (0.18), 407 (sh, 0.027), 526 (sh, 0.055), 550 (0.082). CD (dist. H_2O (+ trace KCN), rel. int.): 306 (−0.82), 317 (sh, −0.61), 330 (−0.28), 340 (−0.34), 360 (sh, 0.072), 376 (1.0), 390 (sh, 0.61), 402 (0.46), 410 (0.49), 445 (0.06), 510 (0.20), 618 (−0.12); $\lambda_0 = 355, 572, 660$. IR (KBr): a.o. 3400*s* (br.), 3110*s*, 3040*s* (br.), 2870*m* (sh), 2140*w*, 2060*w* (br.), 1640*s*, 1560*s*, 1505*s*, 1450*s*, 1395*m*, 1345*m*, 1275*m*, 1225*s*, 1110*s*, 830*s*, 710*m*. ^{1}H-NMR (400 MHz, D_2O): 0.99 (*s*, Me−C(7)); 1.40 (*s*, *β*-Me−C(12)); 1.64 (*s*, Me−C(17)); 1.65 (*s*, *α*-Me−C(12)); 1.72 (*s*, Me−C(2)); 1.87 (*s*, Me−C(1)); 2.44 (*s*, Me−C(5)); 2.59 (*s*, Me−C(15)); superimposed by 1.02–2.90 (*m*, total 24 H); a.o. 1.61 (H−C(2^2), H−C(13^1)), 1.92 (H′−C(2^2), H′−C(13^1)), 2.18 (H−C(17^2)); 2.23 (H′−C(2^1)), 2.31 (H−C(17^1)), 2.41 (H−C(8^1)), 2.46 (CH_2(3^1)), 2.60 (CH_2(13^2)), 2.72 (H′−C(8^1)), 2.78 (*C*H_2(18^1)), H′−C(17^1), H′−C(17^2)); 3.28 (*t*-like, $J \approx 10$, H−C(18)); 3.55 (*d*-like, $J \approx 5$, H−C(3)); 3.59 (*t*-like, $J \approx 5$, H−C(13)); superimposed by 2.90–3.80 (*m*, total 2 H); 3.0 (H−C(8^3)), 3.60 (H′−C(8^3)); 3.87 (*m*, H−C(8)); 4.43, 4.48, 4.55, 4.57 (4*s*, 5 Me-bpy); superimposed by 4.60 (*m*, H−C(7^2)); 4.80 (*s*, H_2O) superimposed by 4.76 (*m*, H′−C(7^2)); 4.87 (*m*, CH_2(3^3)); 4.98 (*m*, CH_2(13^3)); 5.05 (*m*, CH_2(17^3)); 5.23 (*m*, H−C(18^2)); 5.31 (*m*, H′−C(18^2)); 8.20–8.37 (*m*, 2 H), 8.39 (*d*-like, $J \approx 6$, 2 H), 8.52 (*d*-like, $J \approx 6$, 4 H), 8.57 (*d*-like, $J \approx 6$, 2 H), 8.60–8.80 (*m*, 10 H; total 5 H−C(3)-bpy, 5 H−C(3′)-bpy, 5 H−C(5)-bpy, 5 H−C(5′)-bpy); 8.98 (*d*-like, $J \approx 7$, H−C(2)-*b*-bpy, H−C(6)-*b*-bpy); 9.06 (*d*-like, $J \approx 7$, H−C(2)-*c*-bpy, H−C(6)-*c*-bpy); superimposed by 8.80–9.20 (*m*, 5 H−C(2′)-bpy, 5 H−C(6′)-bpy); 9.26 (*d*-like, $J \approx 6$, H−C(2)-*g*-bpy, H−C(6)-*g*-bpy); 9.34 (*d*-like, $J \approx 6$, H−C(2)-*e*-bpy, H−C(6)-*e*-bpy); 9.43 (*d*-like, $J \approx 6$, H−C(2)-*f*-bpy, H−C(6)-*f*-bpy). Selected ^{1}H,^{1}H correlations (H,H-COSY): CH_2(2^1)/CH_2(2^2); CH_2(2^2)/H−C(18). Selected ROE's (ROESY): CH_3−C(1)/H−C(18); CH_3−C(2)/H−C(2)-*g*-bpy; H−C(3)/CH_2(2^1); CH_3−C(17)/CH_2(18^2), H−C(6)-*g*-bpy; H−C(18)/CH_2(18^2), CH_3−C(1); CH_2(18^1)/CH_2(2^2); H−C(2)-*g*-bpy/CH_2(18^2). ^{13}C-NMR (100.6 MHz, D_2O): 17.14 (*q*, *C*H_3−C(5)); 18.33 (*q*, *C*H_3−C(15)); 19.88 (*q*, *C*H_3−C(2)); 22.27 (*q*, *C*H_3−C(17)); 23.83 (*q*, *C*H_3−C(7)); 24.43 (*q*, *α*-*C*H_3−C(12)); 27.61 (*q*, *C*H_3−C(1)); 30.74 (*q*, *β*-*C*H_3−C(12)); 22.69, 24.31, 28.09, 28.59, 29.85, 30.95, 33.25, 34.81, 39.04, 42.09, 43,95 (11*t*, 13 CH_2); 44.56 (*d*, C(18)); 51.27, 51.31 (2 C), 51.34 (2 C) (3*q*, 5 *C*H_3-bpy); 50.86, 51.79, 53.56 (3*s*, C(2), C(7), C(12)); 55.07 (*d*, C(8)); 58.96 (*d*, C(13)); 61.30 (*d*, C(3)); 61.52 (*s*, C(17)); 60.91, 62.58 (2*t*, C(7^2), C(18^2)); 64.18, 64.37, 64.69 (3*t*, C(3^3), C(13^3), C(17^3)); 80.06, 85.90 (2*s*, C(1), C(19)); 107.81, 108.04, 108.11 (3*s*, C(5), C(10), C(15)); 128.68, 129.51, 129.68, 129.71, 129.78, 130.19, 130.24, 130.38 (8*d*, 5 C(3)-bpy, 5 C(5)-bpy, 5 C(3′)-bpy, 5 C(5′)-bpy); 148.26, 148.44, 148.47, 148.56, 148.64, 149.09, 149.19, 149.26 (8*d*, 5 C(2)-bpy, 5 C(6)-bpy, 5 C(2′)-bpy, 5 C(6′)-bpy); 152.34, 152.38, 152.52, 152.57, 152.92, 153.00, 153.29, 153.35, 153.37 (9*s*, 5 C(4)-bpy, 5 C(4′)-bpy); 165.05, 167.65, 173.03, 177.69, 178.05, 180.45 (6*s*, C(4), C(6), C(9), C(11), C(14), C(16)).

4.10. Co*α* (or Co*β*)-*Aqua* (or *Dimethylformamido*)-Co*β* (or Co*α*)-*perchlorato*{*2^1,2^2,8^2,8^3-tetrahydro-7,18-bis-[2-(1′-methyl-4,4′-bipyridinio)ethyl]-3,13,17-tris[3-(1′-methyl-4,4′-bipyridinio)propyl]-1,2,5,7,12,12,15,17-octamethyl-8^1*H-*benzo[*hi*]cyclopenta[*as*]corrinato*}*cobalt(III) Decaperchlorate* (**7b**). A soln. of **7a** (4 mg) dissolved in a minimum amount of H_2O was precipitated upon addition of a few drops of aq. sat. $NaClO_4$ soln. The flocky compound was dissolved in 0.075M $(Bu_4N)ClO_4$ in H_2O/DMF 1:1 (20 ml) and was electrochemically reduced in the spectroelectrochemical cell at −1.0 V (*vs.* SCE) under Ar until the soln. turned colorless. The completely reduced complex did precipitate onto the electrode surface (carbon felt). Under strict exclusion of O_2, the CN^--contaminated solvent/electrolyte was replaced with fresh O_2-free solvent/electrolyte. The surface-bond complex was oxidized at −0.2 V and dissolved in accordance with coulometry. The above procedure was repeated 4 times. The last oxidation was conducted either at −0.2 V or +0.5 V in order to produce s soln. of $Co^{II}-5V^{2+}$ or $Co^{III}-5V^{2+}$, respectively. The soln. was concentrated (high vacuum, 50°) to 5 ml and the residue again diluted with 5 ml of DMF (for CV) or with 0.025M $(Bu_4N)ClO$/DMF to 20 ml (for spectroelectrochemistry).

Using a soln. of 0.063M KBr in H_2O/DMF 1:1 as electrolyte/solvent system, **7a** (4 mg) was transformed into the corresponding $Co^{II}-V_5^{2+}$ undecabromide which, after complete solvent evaporation, was directly checked for CN^- contamination by IR. The typical cyanide resonance at 2140 cm^{-1} was not present.

REFERENCES

[1] a) R. Cosmo, C. Kautz, K. Meerholz, J. Heinze, K. Müllen, *Angew. Chem.* **1989**, *101*, 638; b) J. Heinze, J. Mortensen, K. Müllen, R. Schenk, *J. Chem. Soc., Chem. Commun.* **1987**, 701.

[2] S.-I. Imabayashi, N. Kitamura, S. Tazuke, K. Tokuda, *J. Electronanal. Chem.* **1988**, *239*, 397.

[3] J. B. Flanagan, S. Margel, A. J. Bard, F. C. Anson, *J. Am. Chem. Soc.* **1978**, *100*, 4248.

[4] J. P. Collman, P. Denisevich, Y. Konai, M. Marrocco, C. Koval, F. C. Anson, *J. Am. Chem. Soc.* **1980**, *102*, 6027.

[5] Review: B. Morgan, D. Dolphin, in 'Synthesis and Structure of Biomimetic Porphyrins', in 'Structure and Bonding', Ed. J. W. Buchler, Springer, Berlin, 1987, Vol. 64, p. 115.

[6] a) N. Kaji, S. Aono, I. Okura, *J. Mol. Catal.* **1986,** *36,* 201; b) P. Leighton, J. K. M. Sanders, *J. Chem. Soc., Chem. Commun.* **1984,** 856; c) S. Aono, N. Kaji, I. Okura, *ibid.* **1986,** 170.

[7] a) G. Blondeel, D. de Keukeleire, A. Harriman, L. R. Milgrom, *Chem. Phys. Lett.* **1985,** *118,* 77; b) S. Noda, H. Hosono, I. Okura, Y. Yamamoto, Y. Inoue, *J. Mol. Catal.* **1990,** *59,* L21.

[8] B. Steiger, E. Eichenberger, L. Walder, *Chimia* **1991,** *45,* 32.

[9] a) L. Werthemann, Dissertation, ETH Zürich Nr. 7623, 1984; b) R. Keese in [9a]; c) C. Caderas, Dissertation, ETH Zürich Nr. 7822, 1987; d) E. M. Sauer, K. Broschinski, L. Ernst, H. H. Inhoffen, *Helv. Chim. Acta* **1981,** *64,* 2257.

[10] IUPAC/IUP, *Pure Appl. Chem.* **1976,** *48,* 497.

[11] a) R. Stepanek, B. Kräutler, P. Schulthess, B. Lindemann, D. Ammann, W. Simon, *Anal. Chim. Acta* **1986,** *182,* 83; b) R. Stepanek, Dissertation, ETH Zürich Nr. 8069, 1987.

[12] Y. Murakami, Y. Hisaeda, T. Ohno, *Bull. Chem. Soc. Jpn.* **1984,** *57,* 2091.

[13] B. Grüning, G. Holze, A. Gossauer, L. Ernst, *Helv. Chim. Acta* **1985,** *68,* 1771.

[14] K. W. Willman, R. W. Murray, *J. Electroanal. Chem.* **1982,** *133,* 211.

[15] H. Maag, Dissertation, ETH Zürich Nr. 5173, 1973.

[16] C. E. D. Chidsey, R. W. Murray, *Science* **1986,** *231,* 25.

[17] R. Scheffold, S. Abrecht, R. Orlinsky, H.-R. Ruf, P. Stamouli, O. Tinembart, L. Walder, C. Weymuth, *Pure Appl. Chem.* **1987,** *59,* 363.

[18] B. P. Branchaud, Y. L. Choi, *J. Org. Chem.* **1988,** *53,* 4639.

[19] S. U. Pedersen, B. Svensmark, *Acta Chem. Scand., Ser. A* **1986,** *40,* 607.

[20] a) D. Lexa, J.-M. Savéant, H. J. Schäfer, K.-B. Su, B. Vering, D.-L. Wang, *J. Am. Chem. Soc.* **1990,** *112,* 6162; b) D. Lexa, J.-M. Savéant, K. B. Su, D. L. Wang, *ibid.* **1987,** *109,* 6464.

[21] a) J. M. Savéant, E. Vianello, *Electrochim. Acta* **1965,** *10,* 905; b) R. S. Nicholson, I. Shain, *Anal. Chem.* **1964,** *36,* 706.

[22] K. L. McLachlan, A. L. Crumbliss, *J. Electroanal. Chem.* **1990,** *295,* 113.

[23] a) Z. Goren, I. Willner, *J. Am. Chem. Soc.* **1983,** *105,* 7764; b) R. Maidan, Z. Goren, J. Y. Becker, I. Willner, *ibid.* **1984,** *106,* 6217.

[24] K. K. Park, C. W. Lee, S.-Y. Oh, J. W. Park, *J. Chem. Soc., Perkin Trans. 1* **1990,** 2356.

[25] Y. Saotome, T. Endo, M. Okawara, *Macromolecules* **1983,** *16,* 881.

[26] T. Endo, K. Ageishi, M. Okawara, *J. Org. Chem.* **1986,** *51,* 4309.

[27] K. Ageishi, T. Endo, M. Okawara, *J. Polym. Sci., Polym. Chem. Ed.* **1983,** *21,* 175.

[28] Organic Synthesis, Ed. A. H. Blatt, J. Wiley, New York, 1943, Coll. Vol. II, p. 171.